FE-0208-T1
Distribution Category UC-90c

STUDIES OF PHENOLIC COMPOUND DECOMPOSITION UNDER SYNTHANE GASIFIER CONDITIONS

FINAL REPORT

John P. Fillo
Michael J. Massey

Departments of Chemical Engineering/
Engineering and Public Policy
Carnegie-Mellon University
Pittsburgh, Pennsylvania 15213

Date Published: October, 1979

PREPARED FOR THE PITTSBURGH ENERGY TECHNOLOGY CENTER
Under Contract EW-78-C-22-0208

TABLE OF CONTENTS

Page

SUMMARY 1

Objectives and Experimental Procedure 1
Major Findings 2
General Conclusions 2

INTRODUCTION 4

Production of Phenolic Compounds During Coal Gasification 4
Characteristics of Phenol Decomposition 4
Present Experimental Program 9

EXPERIMENTAL APPARATUS AND PROCEDURE 10

Experimental Apparatus 10
  Reactant Feed System 10
  Thermal Decomposition Reactor 12
  Product Collection System 12
Experimental Procedures 14
  Homogeneous Gas Phase Ortho-Cresol Decomposition 15
  Heterogeneous Fixed Bed Phenol Decomposition 15
Analytical Procedures 17
  Analysis for Phenols 17
  Solids Analyses 18

EXPERIMENTAL RESULTS 18

Homogeneous Gas Phase Decomposition of Ortho-Cresol 23
  Effect of Temperature and Vapor Residence Time on Ortho-Cresol Decomposition 23
  Characteristics of Ortho-Cresol Decomposition 26
  Heterogeneous Decomposition of Phenol 27

DISCUSSION OF RESULTS 29

Mechanisms Influencing the Decomposition of Phenolic Compounds 29
  Thermal Cracking of Phenols 30
  Thermal Hydrocracking of Alkyl Phenols 32
  Thermal Decomposition of Alkyl Benzenes 34
  Decomposition Characteristics of Unsubstituted Aromatic Hydrocarbons 35

TABLE OF CONTENTS (Cont'd)

Page

Kinetics of Homogeneous Gas Phase Decomposition of Ortho-Cresol 36
Characteristics of Heterogeneous Fixed Bed Phenol Decomposition 42
Phenolic Compound Decomposition Patterns 48
  Relative Reactivity of Phenols 50
  Phenolic Compound Decomposition Pathways 51
Application of Results to Coal Gasification Processes 53
Future Related Studies 58

ACKNOWLEDGEMENTS 59

NOMENCLATURE 61

REFERENCES 62

APPENDIX A - Summary of Data from Bench-scale Decomposition Studies 65

APPENDIX B - Non-isothermal Reaction Kinetics for Previous PERC Phenol Decomposition Studies 75

LIST OF TABLES

Table No.	Title	Page
1	Summary of Ranges of Phenolic Compound Production from Coal Gasification Processes	5
2	Summary of Coal Gasification Pilot Plant Operating Conditions	6
3	Thermal Decomposition Reactor Operating Statistics: Homogeneous Gas Phase Decomposition of Phenols	19
4	Thermal Decomposition Reactor Operating Statistics; Decomposition of Phenol in Fixed Beds of Char and Limestone Acceptor Solids	20
5	Summary of Statistical Parameters for Kinetic Evaluation of Ortho-Cresol Decomposition	41
6	Comparative Rate Constants for Homogeneous Gas Phase Decomposition of Phenol and Ortho-Cresol	45
7	Comparative Rate Constants for Thermal Decomposition of Phenol During Homogeneous Gas Phase and Heterogeneous Fixed Lignite Char Bed Reaction	45
8	Comparison of Representative Properties of Lignite and Subbituminous Chars	47
9	Summary of Phenolic Compound Decomposition Over Fixed Beds of Subbituminous Char During Run PDR-73	49
10	Process Conditions Which Affect Production of Phenols for the CO_2-Acceptor, Hygas and Synthane PDU Gasifier	55
11	Phenol Production Patterns for the CO_2-Acceptor, Hygas and Synthane PDU Gasifiers	57
A1	Summary of Measured Reaction Gas Compositions for Homogeneous Gas Phase and Heterogeneous Fixed Bed Phenolic Compound Decomposition Experiments	66

LIST OF TABLE (Cont'd)

Table No.	Title	Page
A2	Summary of Representative Char Analyses	70
A3	Representative Composition of Major Ash Constituents for Lignite and Subbituminous Chars	71
A4	BET Surface Area of Solids Used During Heterogeneous Fixed Bed Phenol Decomposition Experiments	72
A5	Summary of Rate Constants for First Order Homogeneous Gas Phse Ortho-Cresol Decomposition	73
A6	Summary of Rate Constants for Pseudo-First Order Heterogeneous Fixed Bed Phenol Decomposition Experiments	74
B1	Comparison of Homogeneous Gas Phase Phenol Decomposition Kinetic Parameters for Isothermal and Non-Isothermal Reaction	77
B2	Summary of Kinetic Data for First Order Homogeneous Gas Phase Decomposition of Phenol	78
B3	Comparison of Current Homogeneous Gas Phase Decomposition Results with Previously Identified Reaction Behavior	79

LIST OF FIGURES

Figure No.	Title	Page
1	Measured Phenol Decomposition as a Function of Average Reactor Temperature for 2,3 and 4 Seconds Nominal Residence Time	8
2	Thermal Decomposition Reactor -- Basic Bench-Scale Equipment Train	11
3	Thermal Decomposition Reactor and Furnace Configuration	13
4	Summary of Gas Balance Deviations	21
5	Summary of Water Balance Deviations	22
6	Summary of Solids and Ash Balance Deviations for Heterogeneous Fixed Char Bed Experimentation	24
7	Measured Ortho-Cresol Decomposition as a Function of Average Reactor Temperature for 2 and 4 Seconds Nominal Residence Time	25
8	Measured Phenol Decomposition Over Fixed Beds of Lignite and Subbituminous Char, and Limestone Acceptor Solids as a Function of Temperature	28
9	Tautomeric Forms of Phenol and Ortho-Cresol During High Temperature Pyrolysis	33
10	Homogeneous Gas Phase Decomposition Pathway for Ortho-Cresol	38
11	Arrhenius Plot for First Order Homogeneous Gas Phase Decomposition of Ortho-Cresol	39
12	Arrhenius Plot for First Order Decomposition of Phenol Over Fixed Beds of Lignite and Subbituminous Char	43
13	Pathways of Phenolic Compound Decomposition in Coal Gasification Processing	52

SUMMARY

Objectives and Experimental Procedure

Phenolic effluents are produced in varying quantities during the gasification of coal. Process operating conditions such as temperature, vapor residence time, reaction environment, coal heating rate and gas-solid contacting (which vary significantly both within and between processes) determine observed production patterns. More specifically, phenolic compounds are very susceptible to thermal and catalytic cracking in the typical gasification environment. The present experimental program was conducted to determine the pattern of phenolic compound decomposition under typical Synthane PDU gasification conditions. Bench-scale experiments were conducted at atmospheric pressure in a steam/synthesis gas atmosphere to study homogenous gas phase ortho-cresol decomposition characteristics, and quantify phenol decomposition in the presence of gasifier solids. The range of conditions covered in these experiments includes:

(1) reactor temperatures from 430 to 930°C at 2 and 4 seconds vapor residence times, for homogeneous ortho-cresol experiments

(2) reactor temperatures from 360 to 590°C at 6 to 12 second vapor residence times for phenol decomposition in the presence of lignite and subbituminous chars from the Synthane PDU, and limestone acceptor solids from the CO_2-Acceptor pilot plant gasifier.

Major Findings

Results of these experimental investigations indicate:

(1) In the range 500 to 800°C, ortho-cresol undergoes substantial decomposition at nominal residence times of 2 to 4 seconds. Decomposition in excess of 99 percent is achieved at a reactor temperature of 825°C.

(2) Phenol is the principal decomposition product of ortho-cresol. Toluene and benzene, potential dehydroxylation products of ortho-cresol, were conspicuously absent from the product spectrum.

(3) In the range 440 to 600°C, phenol undergoes substantial decomposition at nominal residence times of 6 to 12 seconds in the presence of lignite char solids. Decomposition in excess of 99 percent is achieved at a reactor temperature of 600°C, fully 350°C less than that required for homogeneous gas phase reaction.

(4) Reaction gas methane content remained stable during the course of both ortho-cresol and phenol decomposition experiments. Similarly, hydrogen and carbon monoxide were stable over the full range of conditions, despite the presence of 50 percent water in the reaction atmosphere.

General Conclusions

Major conclusions drawn from this study regarding the decomposition characteristics of phenols are:

(1) Phenols typically formed during coal gasification decompose via successive dealkylation of higher phenol homologues (i.e., xylenols and cresols).

(2) The rate limiting step in the decomposition of phenols during coal gasification is decomposition of the compound phenol.

(3) The presence of char solids in the Synthane PDU, and for that matter other gasification processes, enhances phenol decomposition rates by 2 to 3 orders of magnitude over those seen during homogeneous gas phase reaction under typical gasifier thermal conditions.

(4) Methane content of the reaction gas is stable under conditions conducive to achieving substantial levels of phenolic compound decomposition.

The first and second conclusions are possible based upon coupling these experimental results with xylenol and cresol decomposition characteristics previoulsy documented in the literature. Char solids present in the gasification environment provide substantial surface area for catalytically enhanced reaction of phenols. Data of the nature generated in this experimental study provides information necessary for projecting phenolic effluent production characteristics from pilot- to commercial-scale facilities, as well as for controlling their production during coal gasification processing.

INTRODUCTION

Production of Phenolic Compounds During Coal Gasification

Production of phenols during the gasification of coal varies significantly, both between and within processes. For example (see Table 1), essentially no phenols are produced by the Bigas, CO_2-Acceptor or Synthane (i.e., utilizing fluidized bed-injection of fresh coal) processes, while significant levels of phenols are present in condensates from the Hygas, Slagging Fixed Bed and Synthane (i.e., utilizing free-fall coal feed) processes. On a macroscopic scale, this behavior can be attributed to differences in temperature vapor residence time, reaction environment (e.g., hydrogen partial pressure), coal heating rate and gas-solids contacting(1). Given the widely different processing concepts represented in Table 1, and thus expected variations in operating conditions (see Table 2), variations in phenolic compound production are not surprising. As a result, it is typically difficult to completely assess the mechanisms governing the production (i.e., formation/decomposition) of phenols during coal gasification on such large scales of experimentation.

Characteristics of Phenol Decomposition

In support of its Synthane process development program, the Pittsburgh Energy Research Center (PERC) conducted a series of experimental investigations into the decomposition characteristics of phenol(9).

Table 1. Summary of Ranges of Phenolic Compound Production from Coal Gasification Processes(a)

Process	Phenol Production, lb/ton MAF coal(b)	
	Commercial Projections, Pre-1975	Other Work, 1975 - Present
Bigas	-(c)	-
CO_2-Acceptor	-	< 0.01
Hygas	1 - 3	1 - 16(d)
Lurgi		
Commercial	14 - 15	-
Westfield Semi-Plant	-	7 - 17
Slagging Fixed Bed	-	10 - 30
Synthane	2 - 3	1 - 12(f)

Footnotes:

(a) Source: Reference 2, except where noted.

(b) Refers to moisture- and ash-free coal.

(c) No data.

(d) Includes data from reference 3.

(e) Sources: References 4-8.

(f) Data obtained from the Synthane PDU gasifier (see reference 1).

Table 2. Summary of Coal Gasification Pilot Plant Operating Conditions

Process	Coal Type(a)	Contacting Geometry	Pressure, atm	Temperature(b), °C	
				Devolatilization(c)	Gasification
Bigas	NR	Entrained Flow	69	925-1200	1650
CO_2-Acceptor	Lignite and Subbituminous	Fluidized Bed	11	815	815
Hygas	NR(d)	Staged Fluidized Beds(e)	69	425-650	870
Slagging Fixed Bed	Lignite and Subbituminous	Fixed Bed	< 30	200	1650
Synthane(f)	NR(d)	Fluidized Bed	< 40	400-700	870

Footnotes:

(a) Coal types include lignite, subbituminous and bituminous, with NR referring to no restrictions.

(b) Temperatures represent averages, accurate to within at least ±10 percent. Wide temperature variations are noted.

(c) Initial temperature condition to which coal is subjected.

(d) Use of bituminous coal requires oxidative thermal pretreatment.

(e) Coal is devolatilized in an upflow entrained-flow riser tube.

(f) Operating conditions are for the Synthane PDU gasifier.

Experiments were performed at atmospheric pressure, at temperature and vapor residence times representative of Synthane PDU operation, to investigate both kinetics and products of phenol decomposition during homogeneous gas phase reaction. These studies indicated that substantial levels of phenol decompositon could be effected with minimal production of heavier hydrocarbon tars and oils. Results of this study are illustrated in Figure 1.

As shown in Figure 1, substantial levels of phenol decompositon occurred in the range 750-900°C at 2 to 4 seconds nominal gas residence times. Decomposition in excess of 99 percent was achieved at a temperature of 975°C, regardless of residence time. The presence of lignite char solids in the reactor reduced the required temperature for achieving 99+ percent decomposition by at least 200°C. Products of phenol decomposition consisted mainly of non-condensible gases (i.e., H_2,CO,CO_2,CH_4), with less than 1 weight percent of decomposed phenol reporting as a heavy hydrocarbon condensate. Under conditions conducive to substantial levels of phenol decomposition, the reaction atmosphere remained stable throughout homogeneous gas phase experimentation, with methane composition remaining stable throughout the full range of conditions tested.

The implications of this behavior are significant. Substantial levels of phenol decomposition are possible under process conditions representative of the Synthane process, and for that matter other gasification processes. However, phenol is only one of many phenolic compounds produced during coal gasification (i.e., including cresols and xylenols, with phenol the single most prevalent compound). As a result it would be useful to know the decompositon characteristics (i.e., kinetics and products) of these other phenols, as information on their behavior

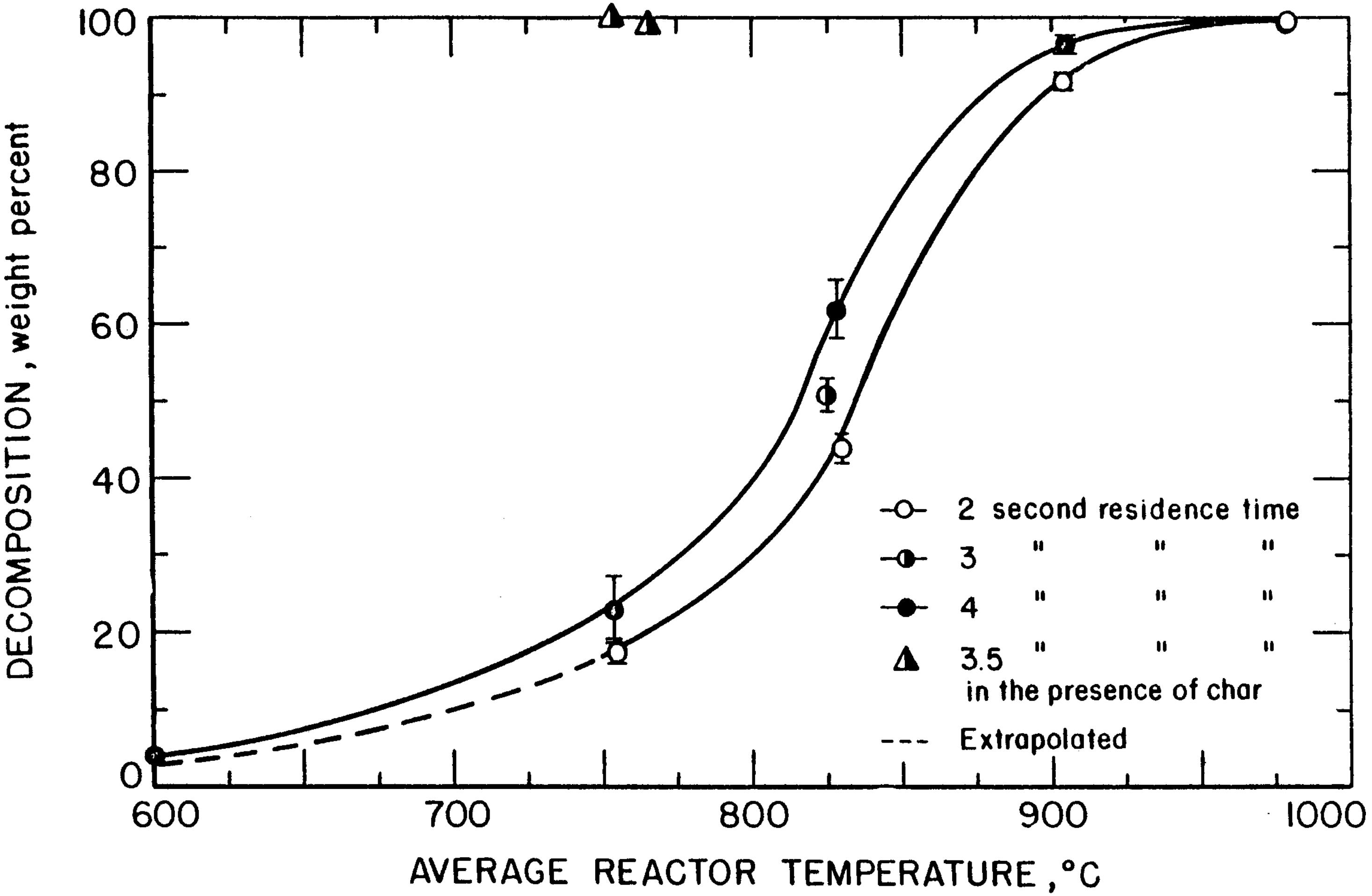

Figure 1. Measured Phenol Decomposition as a Function of Average Reactor Temperature for 2, 3 and 4 Seconds Nominal Residence Time.

under typical coal gasification conditions is not available.

Present Experimental Program

The present experimental program was designed to examine the decomposition characteristics of phenolic compounds under Synthane PDU conditions. Since phenol is but one of many phenols produced during coal gasification, it was important to assess the relative reactivity of select phenols and characteristics of their decomposition products. In addition, the presence of significant quantities of hot char solids during gasification required a more quantitative understanding of the effects of these solids in enhancing phenol decomposition rates. Understanding the pathways of phenolic compound decomposition in the complex coal gasification environment is essential to properly assessing their behavior in pilot-scale facilities and projecting their behavior in prospective commercial-scale designs currently under development.

Effects of various combinations of temperature and residence time (i.e., typical of Synthane PDU operation) on homogeneous gas phase ortho-cresol decomposition were measured in a simulated Synthane PDU gasifier gaseous environment. Decomposition of phenol was studied over fixed beds of North Dakota lignite and Montana Rosebud subbituminous chars, and limestone acceptor solids in a simulated Synthane PDU environment. Results were evaluated in the context of previous studies conducted on the thermal cracking of phenols and other aromatic hydrocarbons.

EXPERIMENTAL APPARATUS AND PROCEDURE

Experimental Apparatus

The apparatus used to conduct these experiments is illustrated in Figure 2. The system consists of three major components: (1) reactant feed, (2) thermal decomposition reactor, and (3) product collection.

Reactant Feed System

Feed materials normally consist of an approximate 1:1 volumetric ratio (at reactor conditions) of reactant gas and water containing ~6000 ppm by weight of the phenolic compound being evaluated. Reactant gases used during the course of experimentation include: (1) pre-blended H_2, CO, CH_4 and CO_2 in the approximate molar ratio 4:1:1:4 (i.e., simulated raw Synthane PDU dry product gas) and (2) nitrogen (also purge gas during reactor startup/shutdown). Reactant gases are stored in separate cylinders, metered with ball float rotameters (i.e., to approximate inlet flowrates) and preheated in 6.35 mm O.D. 304 stainless steel tubing in transit to the reactor. Separate metering systems are provided to enable the adjustment of hydrogen and/or steam partial pressures in the reactor.

Phenolic feed water is stored in a 500 ml. glass buret and delivered to the reactor through a variable flow (i.e., 15-750 ml./hr.) stainless steel bellows pump. A second buret provides distilled water for startup and shutdown of the apparatus during most of the experiments (i.e., homogeneous ortho-cresol decomposition). Water drawn from these

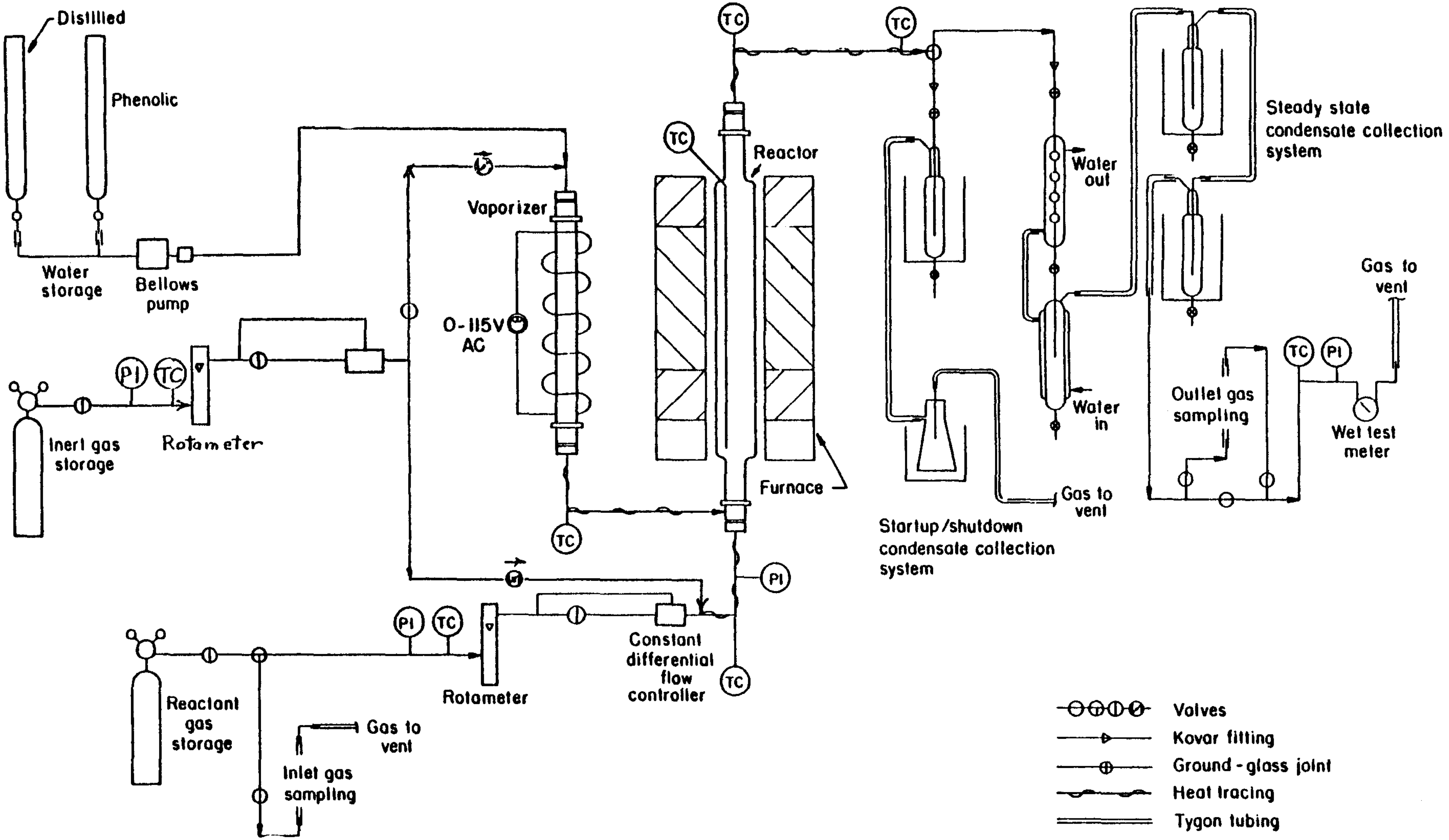

Figure 2. Thermal Decomposition Reactor -- Modified Benchscale Equipment Train.

burettes is vaporized in a 406 mm. x 30 mm. O.D. Vycor glass tube packed with 6 mm. Pyrex glass beads and heated with 24 ga. nichrome resistance wire. Vaporized water is transmitted to the reactor in heated 6.35 mm. O.D. 304 stainless steel tubing. Equal volumes of phenolic feed water samples are taken prior to and after the steady state run, and combined for analysis.

Thermal Decomposition Reactor

The thermal decomposition reactor is illustrated in detail in Figure 3. It consists of a 508 mm. x 57 mm. I.D. Vycor tube reduced in diameter and connected to reactant feed and product collection systems with 37 mm. I.D. stainless steel caps, sealed with silicone rubber o-rings. A 6 mm. O.D. thermocouple well is situated approximately 13 mm. from the inside wall of the reactor, and equipped with a 1020 mm. x 1.0 mm. O.D. slide wire Type K thermocouple.

Reactor temperatures are regulated via manual control of individual zone heat duties in a 570 mm. x 70 mm. I.D. three zone electric furnace. A copper cooling coil on the outlet reactor neck provides cooling to prevent deterioration of the silicone rubber o-rings (i.e., 250-275°C temperature limit). Reactor ends are sealed at the furnace with ceramic wool to prevent air flow through the annular space between reactor and furnace.

Product Collection System

Two product collection systems are provided, one for use

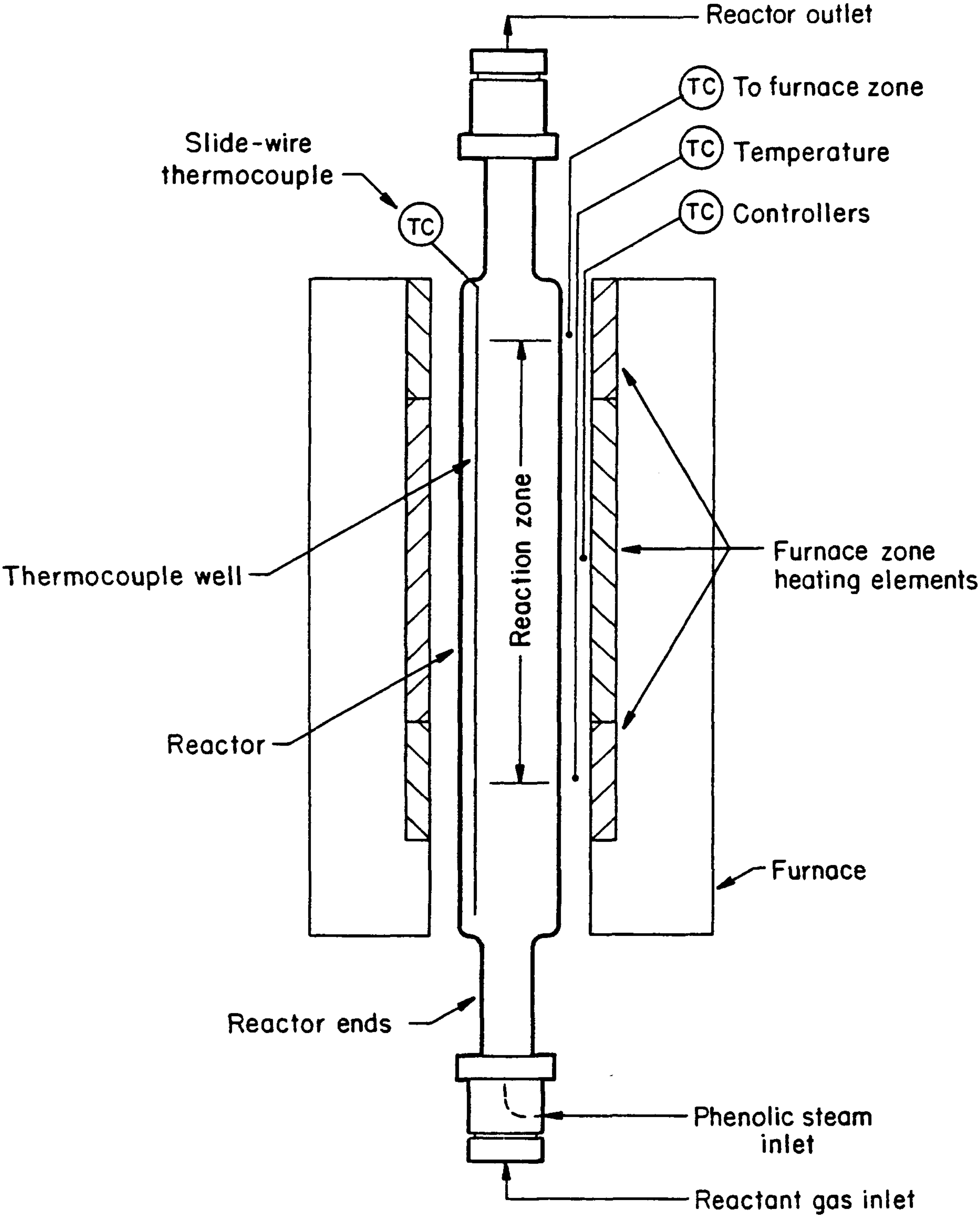

Figure 3. Thermal Decomposition Reactor and Furnace Configuration.

during apparatus start-up and shut-down, the other for sampling during steady state operation. Collection equipment for start-up/shut-down operatins consists of two ice-cooled glass traps. The equipment train for steady state operation consists of two glass water-cooled condensers in series with two ice-cooled glass traps. Reactant gas samples are typically collected before and after steady state operation, with product gas samples, typically three, collected at regular intervals during steady state operation.

Experimental Procedures

Experimental procedure was standardized as much as possible for all runs. Gas sampling bombs, start-up and steady state condensate sampling systems, reactor, vaporizer, and reactant gas feed lines were purged with nitrogen prior to each run. Distilled water feed was started to the reactor after appropriate temperatures were achieved in both vaporizer and reactor. Reactant gas was fed to the reactor only after each of the reactor's zone target temperatures was achieved, as measured in the reactor at the center of each furnace zone. Heating tape settings were monitored frequently to prevent condensation of water in the reactor's inlet and outlet lines, and overheating of the silicone rubber o-rings. System temperatures were continuously monitored by a 12 point chart recorder (i.e., range 0-1000°C), and were manually recorded periodically throughout each run.

Homogeneous Gas Phase Ortho-Cresol Decomposition

Homogeneous gas phase experimentation was conducted using primarily ortho-cresol. During the bulk of these experiments distilled water was replaced with phenolic water as reactor feed when a defined reactor temperature profile was achieved, provided all other system components were functioning smoothly. In a few cases, phenolic water was used throughout the experiment. Reactor outlet was switched to the steady state system when phenolic water reached the vaporizer, this time estimated based on individual run flowrates and feed line liquid holdup (i.e., nominal time delay in the feed line of 30 minutes at 80 cc./hr. and 15 minutes at 160 cc./hr.). Steady state operation typically continued until a minimum of 150 ml. of phenolic water was fed through the reactor. Feed water was replaced with distilled water, and the steady state portion of the experiment terminated after all phenolic water in the feed lines was processed through the vaporizer. Reactor products were switched back to the start-up system at the completion of the steady state run. Reactant gas and distilled water were replaced with nitrogen, and the system was cooled down. Three experiments were conducted using phenol to assess experimental technique relative to the initial series of phenol decomposition experiments(9).

Heterogeneous Fixed Bed Phenol Decomposition

Several experiments were conducted to ascertain the potential catalytic effect of gasifier solids on the decomposition of phenol.

Experiments were conducted in the presence of beds of North Dakota lignite and Montana Rosebud subbituminous chars from the Synthane PDU, and reconstituted limestone acceptor solids from the CO_2-Acceptor pilot plant. In each experiment the reactor contained a 25.0 cm. deep bed of solids supported within the central furnace zone by a bed of 6.35 mm. O.D. inert ceramic balls (Norton Co.). Quartz fiber was used to separate the ceramic supports and the solids bed. Experimental procedures were not altered except to feed phenol-bearing water during both start-up and steady state portions of the run.

Solids used in these experiments were prepared in the following manner:

- North Dakota lignite char was a composite from Synthane PDU tests CHPFL-2,131,147 and 182, screened to remove particles smaller than 100 mesh
- Montana Rosebud char was obtained from Synthane PDU run CHPM-365, screened to remove particles smaller than 100 mesh
- limestone Acceptor solids were obtained from CO_2-Acceptor plant run 47B and screened to remove particles smaller than 20 mesh.

Removal of fines from the char facilitated reducing excessive reactor pressure drop and loss of fines during reactor packing. Removal of particles from acceptor solids (i.e., mostly char) was necessary to ensure proper interpretation of acceptor catalytic effects (i.e., char surface area over 100 times greater than the acceptor). One experiment was conducted feeding wastewater (i.e., containing the full spectrum of phenolic compounds) from Synthane PDU run CHPM-365 to assess the catalytic effects of char on decomposition of the full range of

Analytical Procedures

Gas chromatographic and mass spectrometric (i.e., discontinued after run PDR-53) analyses were performed on all steady state reactant and product gas samples to monitor feed composition, changes in composition due to reaction (e.g., methane decomposition, water-gas shift) and accumulations of phenol decomposition products. Decomposition of phenols was monitored by measuring levels of phenols and total organic carbon (TOC) in steady state reactor feed water and product condensate samples.

Analysis for Phenols

Two procedures were utilized for the analysis of aqueous phenols in this experimental study:

(1) direct ultraviolet analysis(10,11)

(2) direct aqueous injection gas chromatography(12,13)

Ultraviolet analysis was used almost exclusively on feedwaters for experiments conducted with ortho-cresol on the basis of its accuracy and simplicity for identification of pure compounds. Product condensates from these experiments were analyzed using direct aqueous injection GC to permit identification of ortho-cresol decomposition products. Direct aqueous injection GC was utilized exclusively during all solids experiments for identification of aqueous phenol, and for homogeneous experiments conducted after PDR-53.

Solids Analyses

Analyses conducted on char solids included:

1. ultimate and proximate analyses for elemental composition
2. analysis of ash for major constituents
3. BET measurements to assess available surface area for reaction.

Properties of the limestone acceptor solids were supplied by Conoco Coal Development Company(14). Summaries of these data appear in Appendix A.

EXPERIMENTAL RESULTS

A total of 31 experiments were conducted, 21 homogeneous gas phase and 10 over fixed beds of gasifier solids. Homogeneous gas phase experiments were conducted in the range of 430 to 930°C, for vapor residence times of 2 to 4 seconds. Heterogeneous fixed solids bed experimental conditions ranged from 360 to 590°C, for 6 to 12 second vapor residence times (i.e., based on superficial gas velocities). All decomposition experiments were conducted in atmospheres of approximately 50 percent water and synthesis gas (except run PDR-68). Relevant operating statistics for each of these experiments are summarized in Tables 3 and 4 for homogeneous and heterogeneous experiments, respectively; gas and water material balances are summarized in Figures 4 and 5,* respectively. Gas

---

*Balances not reported for (1) PDR-44 and 57 due to spillage of product condensate, (2) PDR-60 due to backup of basic gas scrubbing solution into cold traps, (3) PDR-62 due to loss of CO_2 to acceptor, and (4) PDR-63 as the rotameter was not in calibration range.

Table 3. Thermal Decomposition Reactor Operating Statistics: Homogeneous Gas Phase Decomposition of Phenols

	Reactant Feedrates				Reactor Conditions		Experimental Results		
Experiments	Gas(a,b), SCFH	Water ml/hr	Phenols, mg/hr	Steady-State Operating Time, min	Mean Temp, °C	Residence Time, sec.(c)	Decompositon, wt.or.mol.%	Total Decomposition of Phenols, mol.%	Conversion(d) mol./mol.O-Cresol Fed
PHENOL DECOMPOSITION									
PDR-55	3.719	86.2	497.0	190	825	5.36	74.7	NA(e)	NA
PDR-58	4.094	86.0	594.3	180	750	5.26	30.2	NA	NA
PDR-68(f)	9.401	85.0	1034.3	180	825	2.80	52.1	NA	NA
ORTHO-CRESOL DECOMPOSITION									
PDR-36	4.095	99.0	536.3	120	756	3.71	88.4	70.9	17.5
PDR-38	3.746	80.5	457.7	120	829	4.02	99.7	92.7	6.9
PDR-39	3.447	69.0	403.0	120	904	4.24	99.9+	99.9+	ND(g)
PDR-40	3.037	79.0	464.1	120	929	4.11	99.9+	99.9+	ND
PDR-42	3.924	92.0	533.3	120	754	3.94	88.3	68.1	20.2
PDR-43	8.256	161.5	952.4	120	753	2.05	60.4	29.5	30.9
PDR-44	7.071	162.5	936.6	120	829	2.06	97.9	80.8	17.1
PDR-45	7.135	153.5	877.9	120	904	1.98	99.8	98.3	1.5
PDR-48	4.595	102.0	566.5	120	604	4.05	31.3	30.5	0.8
PDR-49	5.252	111.5	628.6	120	528	3.97	33.3	33.1	0.2
PDR-50(h)	5.839	124.0	694.0	120	478	3.81	99.3	<0	>100
PDR-51	6.138	127.0	750.3	120	429	3.93	35.8	35.6	0.2
PDR-52	8.860	190.0	1123.7	120	680	1.97	43.9	38.0	5.9
PDR-53	9.318	202.0	1199.5	60	604	2.02	36.9	36.6	0.4
PDR-56	4.372	90.3	560.3	180	701	3.98	57.3	42.7	14.6
PDR-57(h)	5.657	108.7	688.4	180	482	4.11	16.4	ND	ND
PDR-69(h)	5.757	115.2	625.4	180	481	3.96	19.7	ND	ND
PDR-70(h)	5.241	109.0	644.6	120	532	4.00	18.1	ND	ND

Footnotes:

(a) SCFH = standard cubic feet per hour at 70°F and 1 atm. pressure as measured by the wet test meter.

(b) All experiments except PDR-68 conducted in the presence of synthesis gas, approximate composition: 40% H_2, 10% CO, 10% CH_4 and 40% CO_2.

(c) Vapor residence time at linear mean temperature within predefined reaction zone (i.e., 0.8971, see Figure 2), except for phenol decomposition experiments (see Appendix B).

(d) Conversion of ortho-cresol to phenol, mol. phenol/mol. o-cresol fed.

(e) Not applicable.

(f) Reaction atmosphere consisted of approximately 55% synthesis gas, 15% nitrogen, and 30% steam.

(g) No detectable phenol in product condensate.

(h) Analytical difficulties apparent in analysis for phenol.

Table 4. Thermal Decomposition Reactor Operating Statistics: Decomposition of Phenol in Fixed Beds of Char and Limestone Acceptor Solids

	Reactant Feedrates				Reactor Operating Conditions(a,b)				
Experiment	Gas(c), SCFH	Water, ml/hr	Phenol, mg/hr	Steady-State Operating Time, min	Mean Temp, °C	Pressure(d), psig	Residence Time(e), sec	Catalytic Solids, gm	Decomposition of Phenol, %
					LIGNITE CHAR SOLIDS				
PDR-59	2.591	52.3	290.5	180	515	4.0	6.81	301	64.1
PDR-60	2.839	50.7	279.8	180	439	(4.8)(f)	7.47	290	9.5
PDR-61	2.489	46.5	253.0	180	588	5.5	7.04	296	99.7
PDR-65(g)	2.355	50.2	310.8	144	490	5.5	7.88	277	45.5
PDR-67	2.857	48.3	299.8	180	361	4.0	8.35	260	32.4
					SUBBITUMINOUS CHAR SOLIDS				
PDR-71	2.380	44.8	252.7	120	513	3.0	7.46	295	30.2
PDR-72	2.711	59.5	352.7	120	436	3.0	6.74	296	-1.9
PDR-73(g)	2.509	46.4	36.3	97	528	(3.0)(f)	7.01	303	NA(h)
					LIMESTONE ACCEPTOR SOLIDS				
PDR-62	1.973	42.3	241.8	180	517	0.5	7.76	973	13.7
PDR-63	1.219	24.4	147.6	240	588	1.5	12.32	896	11.2

Footnotes:

(a) Operating conditions within 25.4 cm. solids bed.

(b) All experiments run in a 50% steam, 50% synthesis gas (see Table 3, footnote 6) atmosphere.

(c) SCFH = standard cubic feet per hour at 70°F and 1 atm pressure as measured by the wet test meter.

(d) Average pressure in 25.4 cm. solids bed.

(e) Residence time in 25.4 cm. solids bed based on superficial gas velocity.

(f) Not recorded, but assumed as average of other char experiments.

(g) Run prematurely ended due to experimental difficulties.

(h) Run performed with wastewater containing phenol, cresols and xylenols from Synthane PDU run CHPM-365.

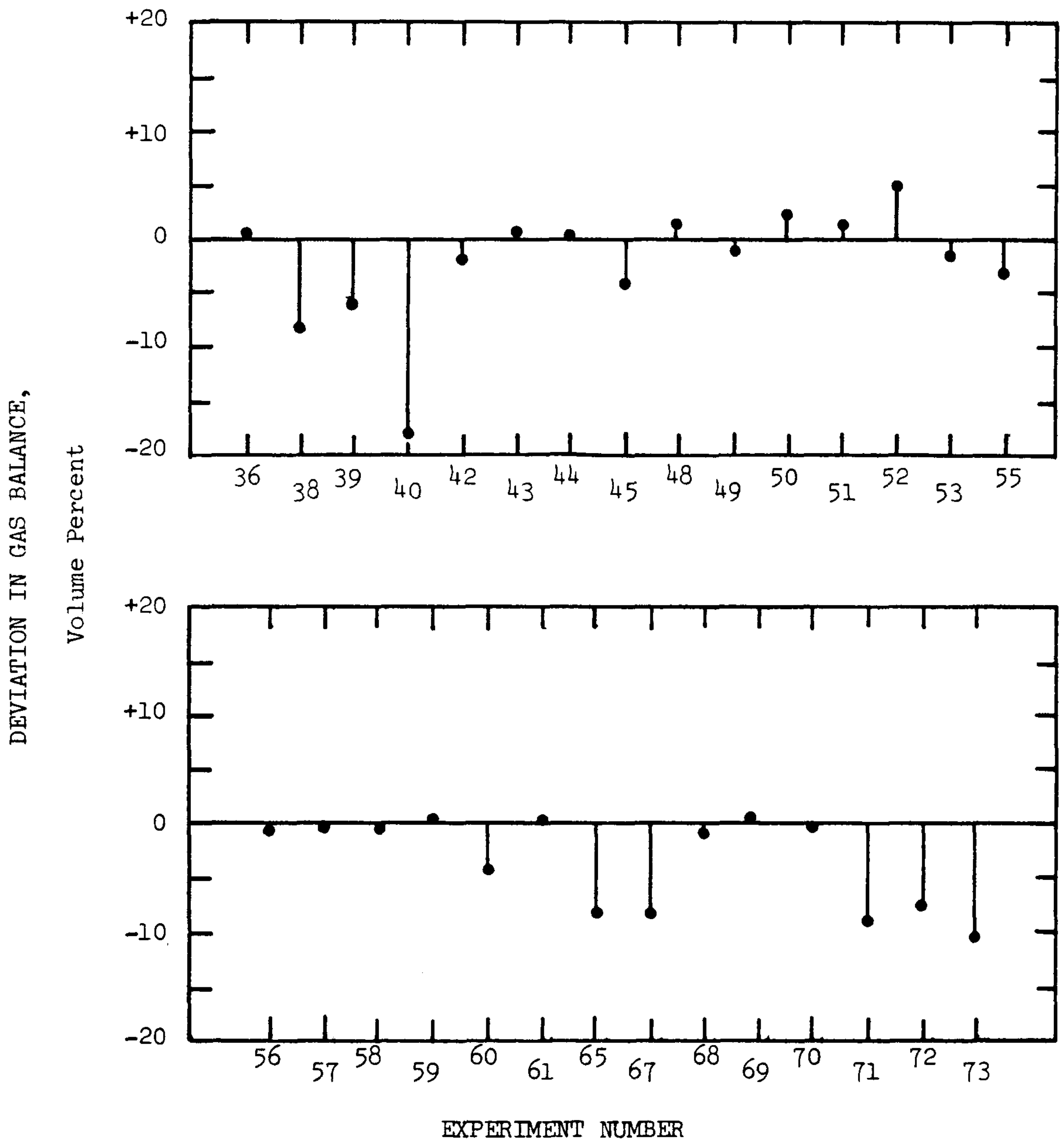

Figure 4. Summary of Gas Balance Deviations.

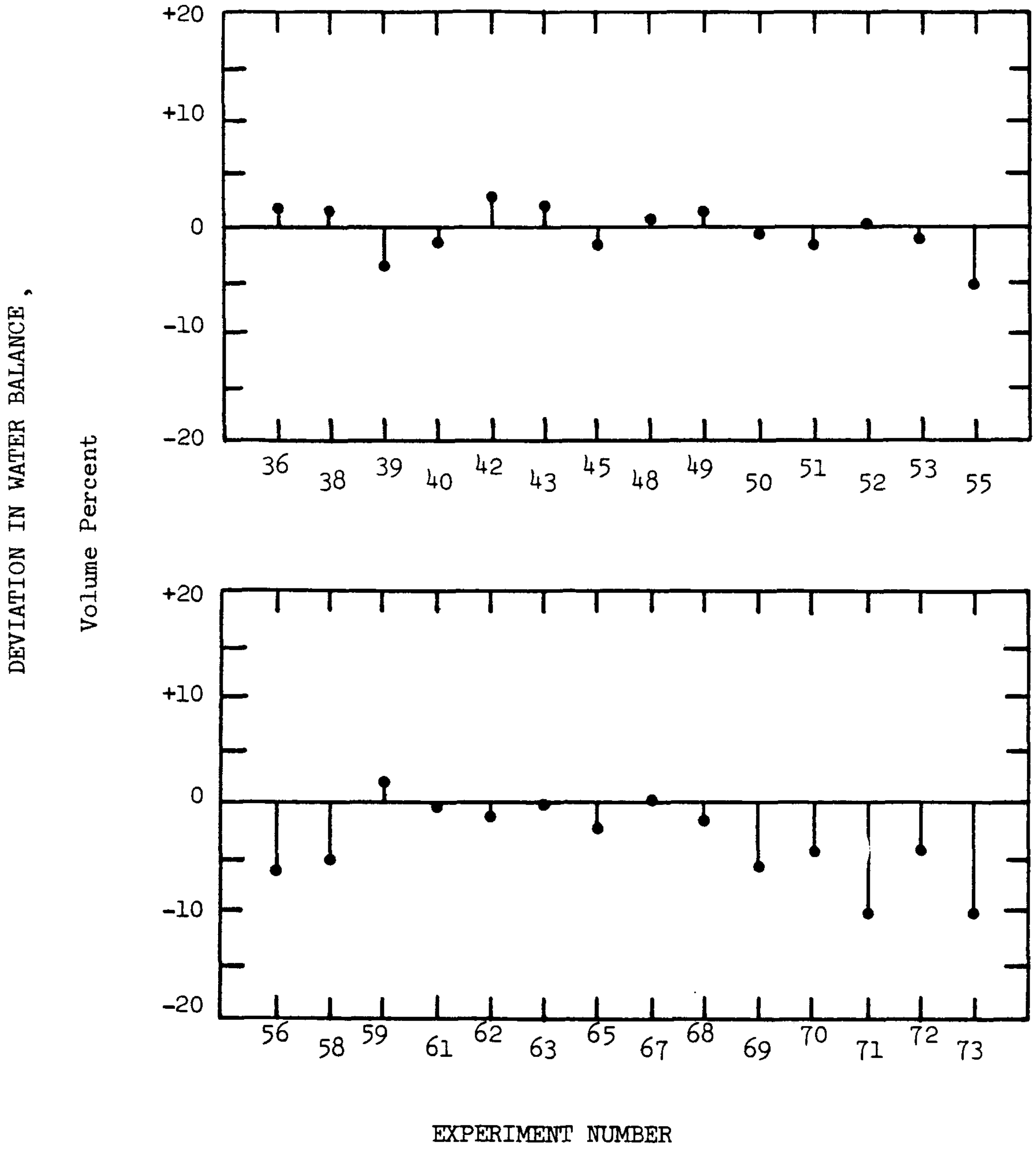

Figure 5. Summary of Water Balance Deviations.

and water balances for homogeneous experiments generally closed within 5 percent, with two thirds of the balances closing within 2 percent. Balances for solids experiments closed within 5 to 10 percent for gas and typically within 5 percent for water. Finally, solids balances for fixed bed char decomposition experiments (i.e., total solids and ash), are summarized in Figure 6. Note that solids balance deviations generally run consistent with ash balance deviations,primarily reflecting loss of material during char handling.

Homogoeneous Gas Phase Decomposition of Ortho-Cresol

Experimental results indicate that substantial amounts of ortho-cresol decomposition are achieved by homogeneous gas phase reaction at 825°C in less than 4 seconds. Significant quantities of tar production and carbon deposition were not visibly noticed. This was not surprising considering that synthesis gas was used exclusively as the reactant gas (i.e., 1:1 mix by volume of water and gas) during these experiments.

Effect of Temperature and Vapor Residence Time on Ortho-Cresol Decomposition

Data showing the relationship of ortho-cresol decomposition to reaction temperature and vapor residence time are illustrated in Figure 7.* Experimental results show a strong dependence of ortho-cresol decomposition

---

*Solids balances not reported for (1) PDR-62 and 63 due to pickup of CO_2 from reaction gas during these experiments, resulting in 2 and 5 percent weight increases, respectively; and (2) PDR-72 and 73, as data were incomplete.

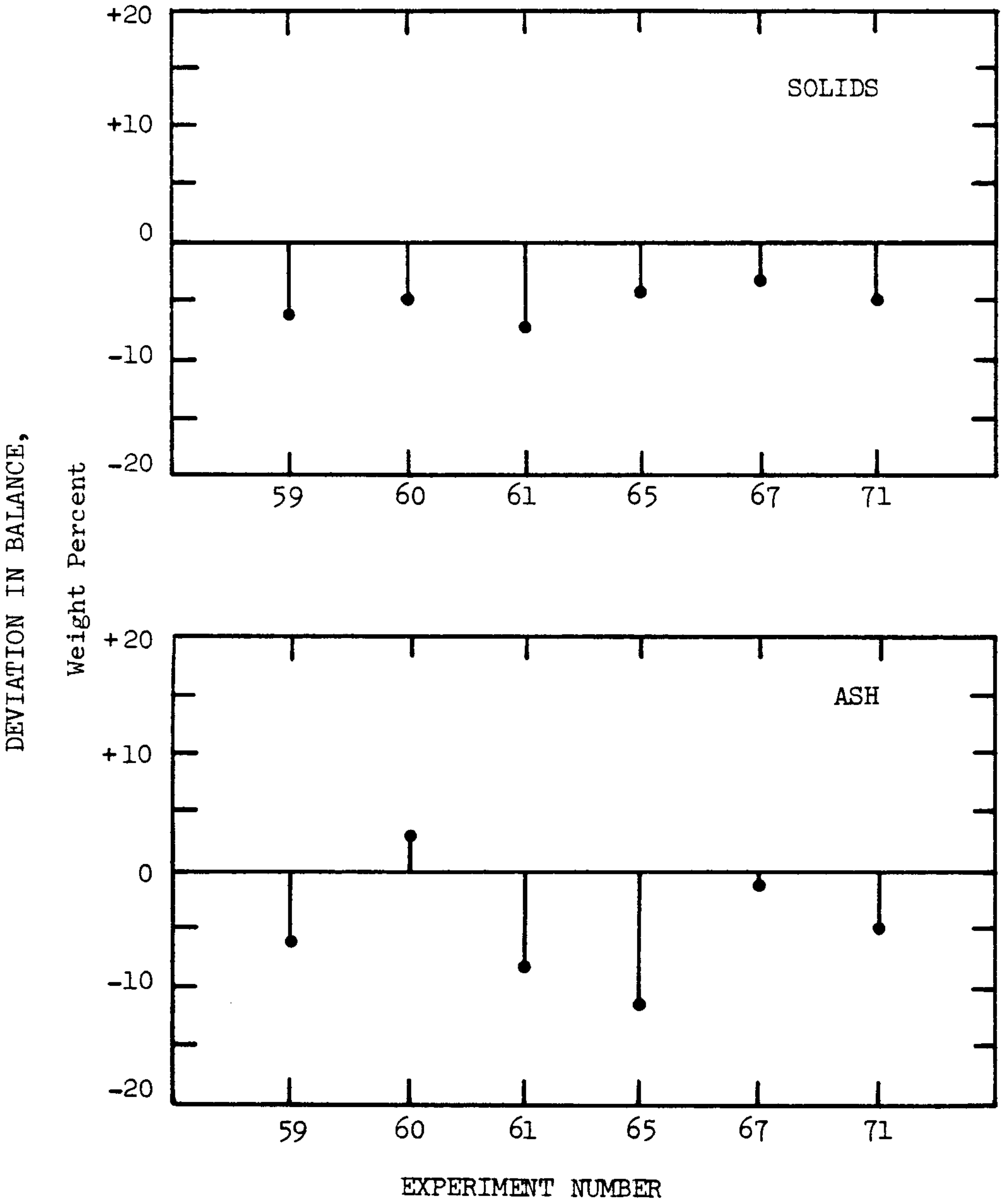

Figure 6. Summary of Solids and Ash Blance Deviations for Heterogeneous Fixed Char Bed Experimentation.

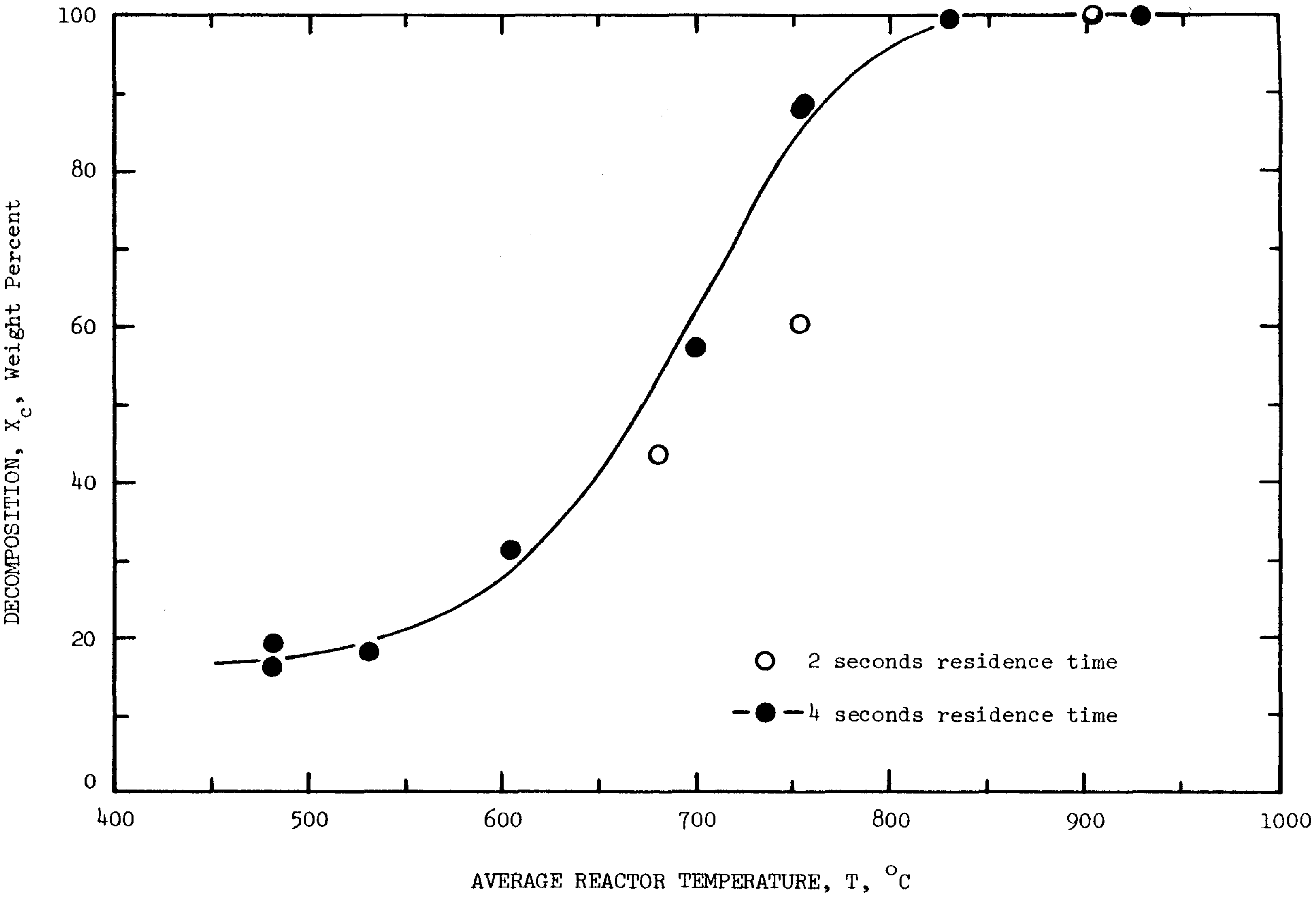

Figure 7. Measured Ortho-Cresol Decomposition as a Function of Average Reactor Temperature for 2 and 4 seconds Nominal Residence Time.

upon both reaction temperature and vapor residence time. Significant increases in decomposition occur at temperatures between 600 and 800°C. The effects of changes in hydrogen partial pressure on the decomposition rates of ortho-cresol are not known, as it was not determined in this experimental program.

Characteristics of Ortho-Cresol Decomposition Products

The single most abundant product of ortho-cresol decomposition was the compound phenol. This was the only compound, other than ortho-cresol, detected in measurable quantities in the product condensate. Conspicuously absent from this condensate were benzene and toluene (i.e., potential dehydroxylation products of ortho-cresol), which were rarely detected other than in trace quantities. Although not quantified in these experiments, no noticeable deposition of carbon or tars was noticed, consistent with results for phenol in a water/synthesis gas atmosphere(9). Similarly, reaction gas composition (see Appendix A) particularly methane, was remarkably stable over the full range of reactor thermal conditions (i.e., conditions causing significant levels of decomposition). This result was consistent with stable methane production yields previously reported for the Synthane PDU(1), and results of previous bench-scale investigations(9).

Heterogeneous Decomposition of Phenol

Experiments conducted to scope the effects of lignite and subbituminous chars, and limestone acceptor solids on the extent of phenol decomposition showed significantly different behavior. Substantially complete decomposition of phenol was found to occur for reaction over a fixed bed of lignite char from the Synthane PDU at temperatures as low as 600°C in less than 6 seconds. By contrast, decomposition of phenol over fixed beds of limestone acceptor showed phenol decomposition only slightly higher than that observed during homogeneous gas phase reaction at the same temperature. Limited experimentation over fixed beds of subbituminous char from the Synthane PDU yielded a somewhat lower decomposition of phenol than in the lignite experiments.

Data on the relationship of phenol decomposition to reaction temperature are shown in Figure 8. The low temperature end of the homogeneous gas phase decomposition curve is shown for comparison. Results of these experiments show a significant effect of char solids on the extent of observed decomposition of phenol. At a reaction temperature of approximately 600°C, essentially complete decomposition of phenol occurs for heterogeneous reaction in the presence of lignite char, fully 375°C less than that seen for the homogeneous case. The effect of limestone acceptor solids is significantly less substantial, with only 11 percent decomposition observed at a temperature where complete decomposition occurs in the presence of lignite char. It is suspected that the high surface are of the chars (i.e., lignite: 360 $m.^2/gm.$;

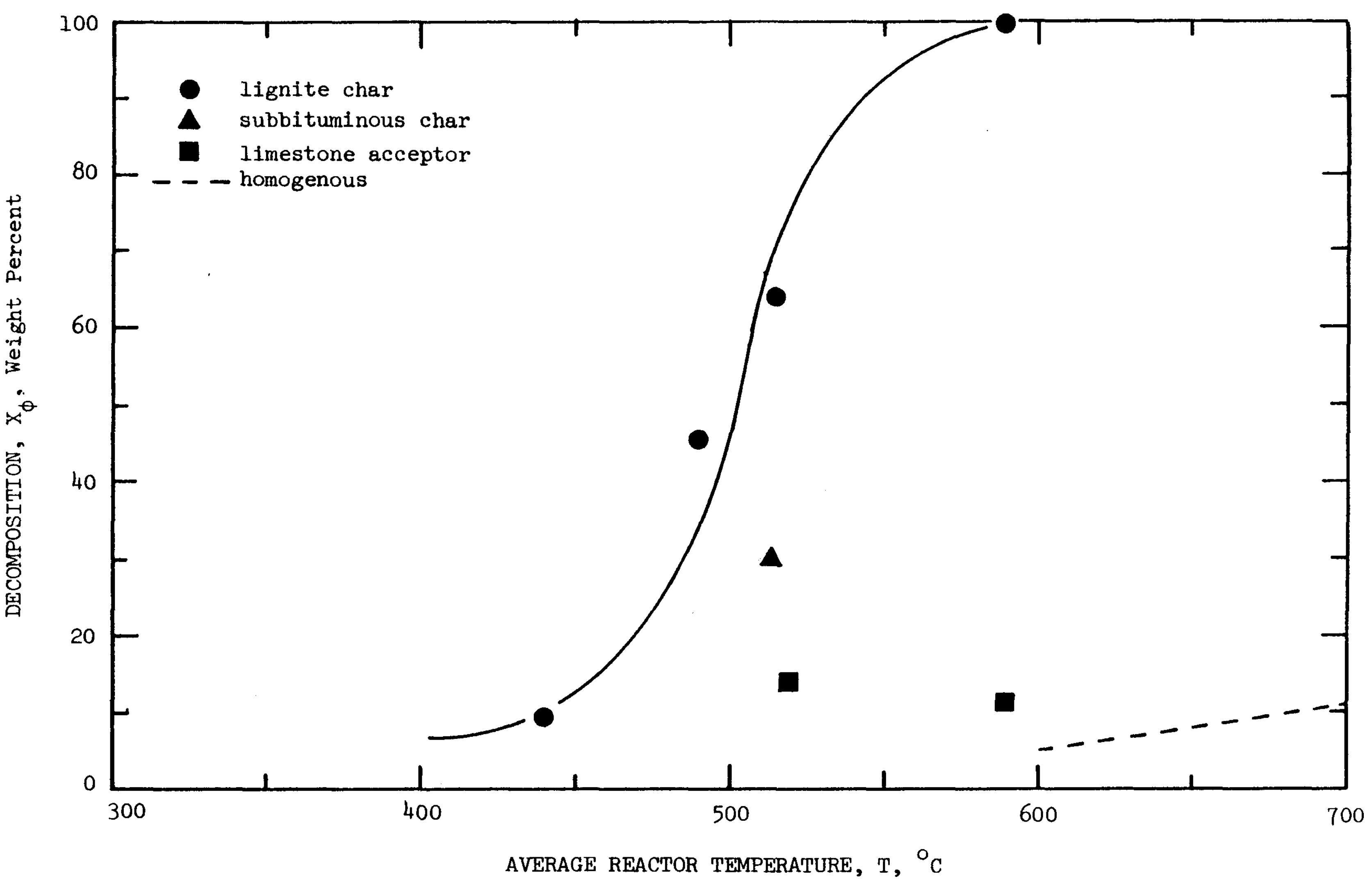

Figure 8. Measured Phenol Decomposition Over Fixed Beds of Lignite and Subbituminous Char, and Limestone Acceptor Solids as a Function of Temperature.

subbituminous: 230 $m.^2/gm$) in contrast to that for the limestone acceptor (i.e., <1 $m.^2/gm.$), is responsible for providing the potential for catalytically enhanced reaction.

DISCUSSION OF RESULTS

Mechanisms Influencing the Decomposition of Phenolic Compounds

Consideration of the full spectrum of phenolic compounds found in coal gasification aqueous condensates presents a multitude of possible reaction pathways leading to their decomposition. The presence of alkyl derivatives (e.g., cresols, xylenols) of phenol suggests possible decomposition pathways of dehydroxylation and dealkylation, in addition to simple aromatic ring decomposition previously identified for phenol under gasification conditions(9). The presence of hydrogen and/or steam could be expected to affect the mechanisms and products of this decomposition. As a result it is appropriate to review the thermal cracking literature with the following aromatic hydrocarbon types in mind:

- Thermal Cracking of Phenols: Background literature available on the thermal decomposition of phenolic compounds in inert atmospheres, until recently, concentrates on the higher phenol homologues (i.e., cresols, xylenols) and provides insights into the initial mechanistic steps that occur during their decomposition. Unfortuantely, these studies are conducted under conditions which are not totally representative of those occurring in coal gasification systems.

- Thermal Hydrocracking of Alkyl Phenols: The presence of hydrogen significantly affects the decomposition characteristics of these compounds. Coal gasification reactors typically contain significant fractions of hydrogen in the product gas. Thus, insights into the decomposition of these compounds in the presence of hydrogen shed significant light upon their behavior in coal gasification reactors.

- Thermal Decomposition of Alkyl Benzenes: A conceivable decomposition pathway for the methyl-substituted phenols is dealkylation. This decomposition mechanism is affected by the presence of hydrogen, and can be paralleled in certain respects to the behavior of alkyl phenols. A brief review of this literature provides information pertinent to delineating the behavior of phenols during coal gasification.

- Decomposition Characteristics of Unsubstituted Aromatic Hydrocarbons: Significant differences exist in the behavior of unsubstituted and substituted aromatic hydrocarbons during thermal decomposition. Primarily, the role of hydrogen is different for each of these classes of compounds. In view of the hydrogen-independent decomposition of phenol previously identified(9), review of these literature sources is appropriate.

An understanding of the characteristics of thermal decomposition of these aromatic compounds is necessary to properly interpret the results of the present experimental studies.

Thermal Cracking of Phenols

Studies of the thermal cracking of alkyl phenols and tar acid fractions were conducted by reacting phenols in a steam carrier over quartz chips between temperatures of 750 and 875°C at residence times of 0.05-0.5 seconds(15,16). A reaction rate model first order in phenolic compound was proposed, and rate constants were calculated. The order of increasing reactivity for the compounds examined was m-cresol, p-cresol, o-cresol, and 2, 4-xylenol. Activation energies calculated from the data were 69, 70, and 75 kcal./gm.mol. for o-cresol, 2,4-xylenol, and m-cresol, respectively. Distribution of product materials included benzene, toluene and phenol, indicating that both demethylation and dehydroxylation of the phenolic compounds occurred.

A study of the thermal decomposition characteristics of isomeric cresols was conducted by passing individual cresols through a variety of reactor tubes (e.g., glass, copper, iron) between temperatures of 700-800°C at specified feed rates(17). Product distributions during these studies were found to vary with isomeric cresol, reactor tube, and time into an experiment. Products included gaseous hydrocarbons, phenol, benzene, toulene and tar, again suggesting both demethylation and dehydroxylation. The reactivity of the isomeric cresols from these data increased in the order meta < ortho < para.

More recent studies on the pyrolysis of phenolic compounds in a nitrogen carrier were conducted for the purpose of identifying intermediate reaction products in the overall scheme of decompositon(18), using phenol and m-cresol at atmospheric pressure between 650 and 850°C, and 0-30 second residence times. Results indicated that both demethylation and dehydroxylation occurred during pyrolysis of m-cresol yielding major products of phenol, benzene, toluene, water and gaseous hydrocarbons. Phenol pyrolysis yielded benzene, water and naphthalene as primary liquid products. A variety of multi-aromatic ring compounds (e.g., fluorene, diphenyl, indene) were formed in small quantities. Results suggested that the pyrolysis processes consisted of both degradation and condensation reactions.

Further studies of these reactions were performed at atmospheric pressure, 2.5 seconds residence time, in the temperature range 665-865°C(19,20). Radioactive labelling of phenols with ^{14}C and ^{3}H in specific positions was used to delineate the possible reaction paths. Initial reaction of phenols appeared to proceed through a tautomeric form of the phenols (see Figure 9). Formation of benzene, and to some extent toluene, occurred directly from the original phenol. Production of other aromatic molecules appeared to occur as a result of condensation of two C_6H_5 fragments. Formation of specific reaction products depended on the molecule eliminated from phenol (e.g., OH, C-O).

Finally, a recent study was conducted on pyrolysis of o-cresol and 2,4-xylenol under vacuum conditions(21). Unfortunately, neither reactor residence time nor gaseous reaction products could be identified. Very low levels of cracking were obtained, with only trace amounts of benzene and toluene detected. A variety of possible reaction mechanisms were proposed, however no concrete conclusions were advanced.

Thermal Hydrocracking of Alkyl Phenols

While the aforementioned studies of phenolic compound pyrolysis are of general interest they are unrealistic in light of typical conditions in coal gasification processing. Significant quantities of hydrogen present in coal gasification reactors can affect the eventual disposition of the decomposition fragments from these molecules. Two studies of this behavior are available, and evaluate the decomposition of cresols and xylenols(22), and cresols(23).

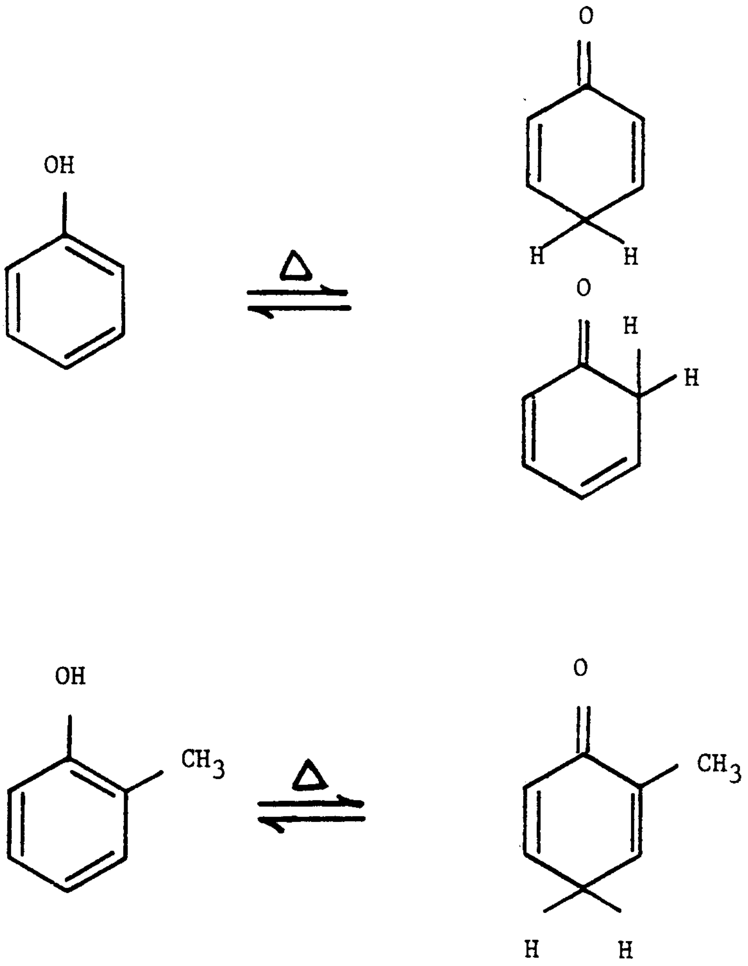

Figure 9. Tautomeric Forms of Phenol and Ortho-Cresol During High Temperature Pyrolysis.

Studies of thermal dealkylation-hydrocracking of cresols and xylenols were performed at 30 atm. pressure, at 600-700°C over a bed of coke(22). Results of these studies provided some interesting insights into the decomposition characteristics of phenols:

- in the presence of hydrogen (i.e., 2:1 molar ratio), primary products of o-cresol decomposition were phenol and toluene
- the order of cresol stability to hydrocracking was meta > para > ortho
- xylenols as a class were more reactive than cresols, with cresols being the primary decomposition product at 600°C and 20 sec. residence time
- tar formation in these experiments was negligible, the bulk being conducted at a H_2:phenolic compound molar ratio of 2:1.

This work continued into a more detailed study of thermal hydrocracking of cresols at pressures up to 390 psig, between 580-700°C and H_2:cresol molar ratios of 0.8:1.0 - 4.0:1.0(23). Experiments were conducted in the homogeneous gas phase in a continuous flow reactor. A 1.5 - order rate equation was fit to the experimental data for H_2:cresol ratios greater than 1:1 to obtain kinetic constants for ortho- and meta-cresols. The order of cresol stability was again found to be meta > para > ortho, for decomposition occurring by both dealkylation and dehydroxylation.

Thermal Decomposition of Alkyl Benzenes

The decomposition kinetics of methyl-benzenes has been a subject of considerable investigation. Studies consist of both pyrolysis and hydrodealkylation of methylbenzenes including toluene isomeric xylenes, and mesitylene. Results of these studies are summarized, and include:

- rate of decomposition is first order in hydrocarbon, and exhibits a dependence on hydrogen partial pressure of 0.5 order (24,25)
- decomposition rates increase in the order toluene< isomeric<xylenes
- reaction rates appear first order in hydrocarbon with no dependence upon hydrogen partial pressure when a large excess of hydrogen is present (i.e., 5:1 molar ratio or greater)(24).

Interestingly enough, this behavior closely parallels that previously identified for cresols, including the apparent independence of reaction rates above a H_2:cresol molar ratio of 5:1(23).

Decomposition Characteristics of Unsubstituted Aromatic Hydrocarbons

A significantly different phenomenon occurs during the decomposition of unsubstituted aromatic molecules. In studying pyrolysis and thermal hydrogasification of aromatic compounds it was found that decomposition rates were substantially independent of hydrogen partial pressures over the range zero (i.e., nitrogen carrier) to 100 atmospheres(27). Experimental kinetic data for benzene and anthracene yielded activation energies that were proportional to their respective delocalization energies. Thus, it was postulated that the rate-determining step was the initial thermal decomposition (i.e., aromatic ring destabilization) of the aromatic molecule, with decomposition rates first order in the aromatic and independent of hydrogen partial pressure. Experimental reaction rates for methyl radical attack of various aromatic compounds were shown to be ordered inversely to calculated delocalization energies, with hydrogen affecting only the formation of final decomposition products.

An important aspect of this mechanistic interpretation of aromatic hydrocarbon decomposition is that the reaction rate should be independent of the products being formed. Further reaction following the rate-determining step in the reaction sequence only affects the types of products formed. Formation of heavy hydrocarbons and carbon are favored in atmospheres starved of hydrogen. Formation of lighter gaseous species are favored in an excess hydrogen atmosphere.

Kinetics of Homogeneous Gas Phase Decomposition of Ortho-Cresol

Experimental ortho-cresol decomposition data indicated that it was significantly more reactive than its lower homologue phenol. Based upon the characteristics of these experiments and previously reported behavior in the literature, the following assumptions were made to evaluate ortho-cresol decomposition data:

(1) due to the presence of excessive amounts of water relative to ortho-cresol in these experiments (i.e., fully 1000:1 on a molar basis), it was assumed that reaction by dehydroxylation was negligible(28,29)

(2) presence of excessive amounts of hydrogen in the reaction gas atmosphere (i.e., fully 300:1 on a molar basis) justifies consideration of ortho-cresol decomposition as a first order reaction for comparative purposes(23,24).

The first assumption implies that ortho-cresol decomposition occurs exclusively through phenol as the sole intermediate product. This was substantiated throughout the experimental program as neither benzene nor toluene were detected in more than trace quantities. The second assumption permits direct comparison of ortho-cresol decomposition rate constants with those previously determined for phenol(9). The assumed reaction sequence is illustrated in Figure 10.

Considering the postulated reaction sequence, the reaction rate of ortho-cresol is expressed as:

$$-r_c = kC_c = k\, C_{co}(1-X_c) \tag{1}$$

which, if assuming an ideal tubular flow reactor,

$$\frac{V}{F_{co}} = \frac{V}{v_o C_{co}} = \int_0^{X_c} \frac{dX_c}{kC_{co}(1-X_c)} \tag{2}$$

This gives an expression for k of the form;

$$k = \frac{v_o}{V} \ln\left(\frac{1}{1-X_c}\right) = \frac{1}{\tau} \ln\left(\frac{1}{1-X_c}\right) \tag{3}$$

First order rate constants (i.e., $\sec^{-1}$) are calculated using equation (3) for experiments conducted from 475 to 975°C nominal reactor temperature, and are plotted in Figure 11 on a logarithmic scale as a function of reciprocal absolute temperature. A least squares linear fit of these data indicates an activation energy of 16.6 ± 0.7 kcal./gm.mol., with a coefficient of determination of 0.93 for the regression line.

Additional assumptions required to perform this kinetic analysis include:

(1) total number of mols of reactants in the system are constant

(2) temperatures used are a linear average of the axial profile of the reaction zone (see Figure 3) recorded during steady state operation

(3) reactor volume is that contained within the pre-defined reaction zone (i.e., 0.897 liters).

The first assumption is appropriate as the number of mols of ortho-cresol is at least two orders of magnitude less than the total number of mols in

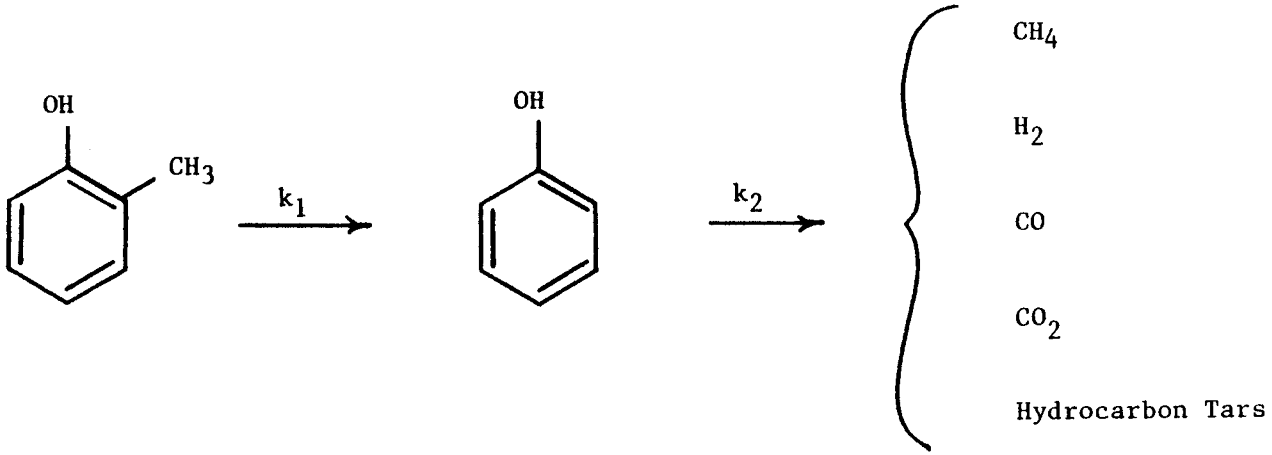

Figure 10. Homogeneous Gas Phase Decomposition Pathway for Ortho-Cresol.

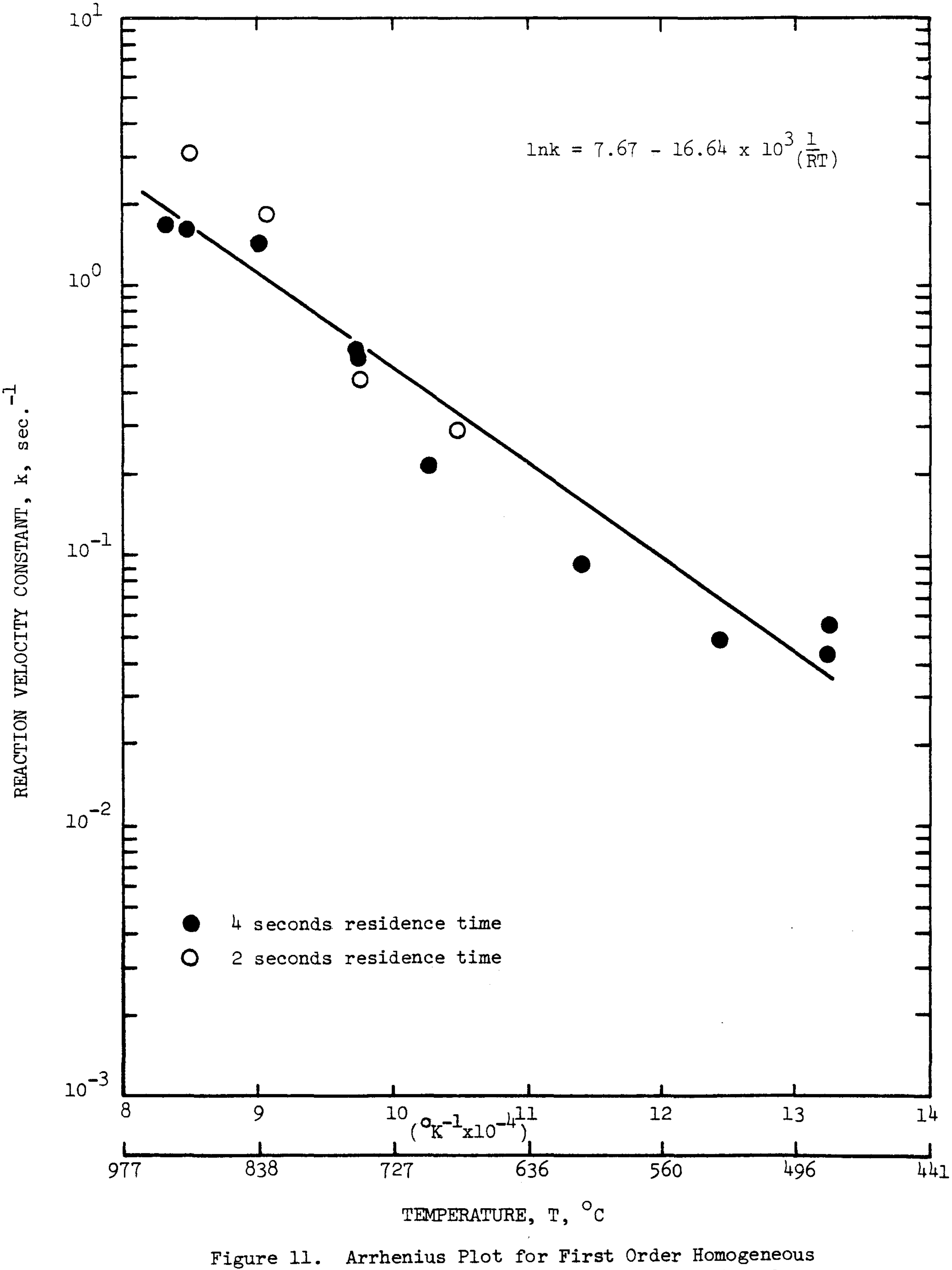

Figure 11. Arrhenius Plot for First Order Homogeneous Gas Phase-Decomposition of Ortho-Cresol.

the system. Reaction temperature/volume assumptions are based on previously demonstrated temperature profile characteristics of this reactor system(9).

Evaluation of these data in light of other reaction mechanisms (see Table 5) shows the following behavior:

(1) rate constants calculated assuming ortho-cresol decomposition as first order in cresol and half-order in hydrogen yield an activation energy of 17.9 ± 0.7 kcal./gmol., with a coefficient of determination of 0.94 for the regression line

(2) calculation of first order rate constants assuming a parallel decomposition pathway to undetermined products yields activation energies of 30.9 and 19.6 kcal./gmol. for first and 1.5 order ortho-cresol decomposition to phenol, respectively.

The first result is not surprising considering behavior demonstrated in previous studies of cresol and toluene hydrodealkylation(23,24). First order rate constants do not vary above a hydrogen:hydrocarbon molar ratio of 5:1. The second point is interesting as activation energies for ortho-cresol decomposition to phenol are more representative of thermal decomposition reactions, but still do not compare well with previously reported kinetic data (i.e., activation energies of 45-50 kcal./gmol.)(22-26) for hydrodealkylation reactions. Previous experimental studies, however, were not conducted in the presence of such excessive quantities of steam (i.e., fully 1000/1 on a molar basis). The presence of steam in the reacting atmosphere may in some way act to accelerate these decomposition reactions while also acting to inhibit dehydroxylation of phenols(28,29), as seen in these experiments.

In light of the available data, especially the lack of data at different hydrogen partial pressures, no definitive statement can be

Table 5. Summary of Statistical Parameters for Kinetic Evaluation of Ortho-Cresol Decomposition(a)

Reaction Mechanism(b)	Activation Energy, kcal/gmol	Frequency Factor, lnA	Coefficient of Determination, r^2
Series - 1st Order (14)	16.6	7.7	0.93
Series - 1.5th Order (14)	17.9	11.3	0.94
Parallel - 1st Order (9)(c)			
To Phenol	30.9	12.8	0.75
Und. Products	24.5	11.2	0.87
Parallel - 1.5th Order (9)(c)			
To Phenol	19.6	10.5	0.73
Und. Products	27.0	15.4	0.90

Footnotes:

(a) Data from runs PDR-49 through 51, and PDR-53, not included.

(b) Values in parentheses indicate number of data points correlated.

(c) Kinetic constants from runs PDR-39,40,57,69 and 70 not available due to lack of detected phenol in product condensates.

made regarding the mechanism of ortho-cresol decomposition. However, based upon the lack of measureable toluene in the reaction products and the large relative amounts of water and hydrogen, decomposition to phenol as the major product occurs by dealkylation. It is of interest to compare the statistically obtained first order rate constants to those obtained for phenol (see Appendix B). Ratios of rate constants at temperatures from 600-900°C (see Table 6) indicate that ortho-cresol is significantly more reactive than phenol at temperatures typical in gasification processing, especially as temperatures approach the lower end of the spectrum. This is supported by the experimental observations reported here.

Characteristics of Heterogeneous Fixed Bed Phenol Decomposition

Results obtained from experiments on phenol decomposition in fixed beds of char solids indicated a substantial acceleration of decomposition rates. In order to quantify the reactivity of phenol in the presence of char, pseudo-first order rate constants were calculated for the lignite experiments based upon superficial gas velocities in the 25.4 cm. char bed, assuming a linear average temperature. First order rate constants were plotted in Figure 12 on a logarithmic scale as a function of inverse absolute temperature for experiments run between 440 and 590°C. A least squares linear fit of these data indicates an activation energy of 33.6 ± 0.6 kcal./gm.mol., with a coefficient of determination of 0.998 for the regression line. It seems fortuitous that this assumed treatment of the data yields such a good correlation,

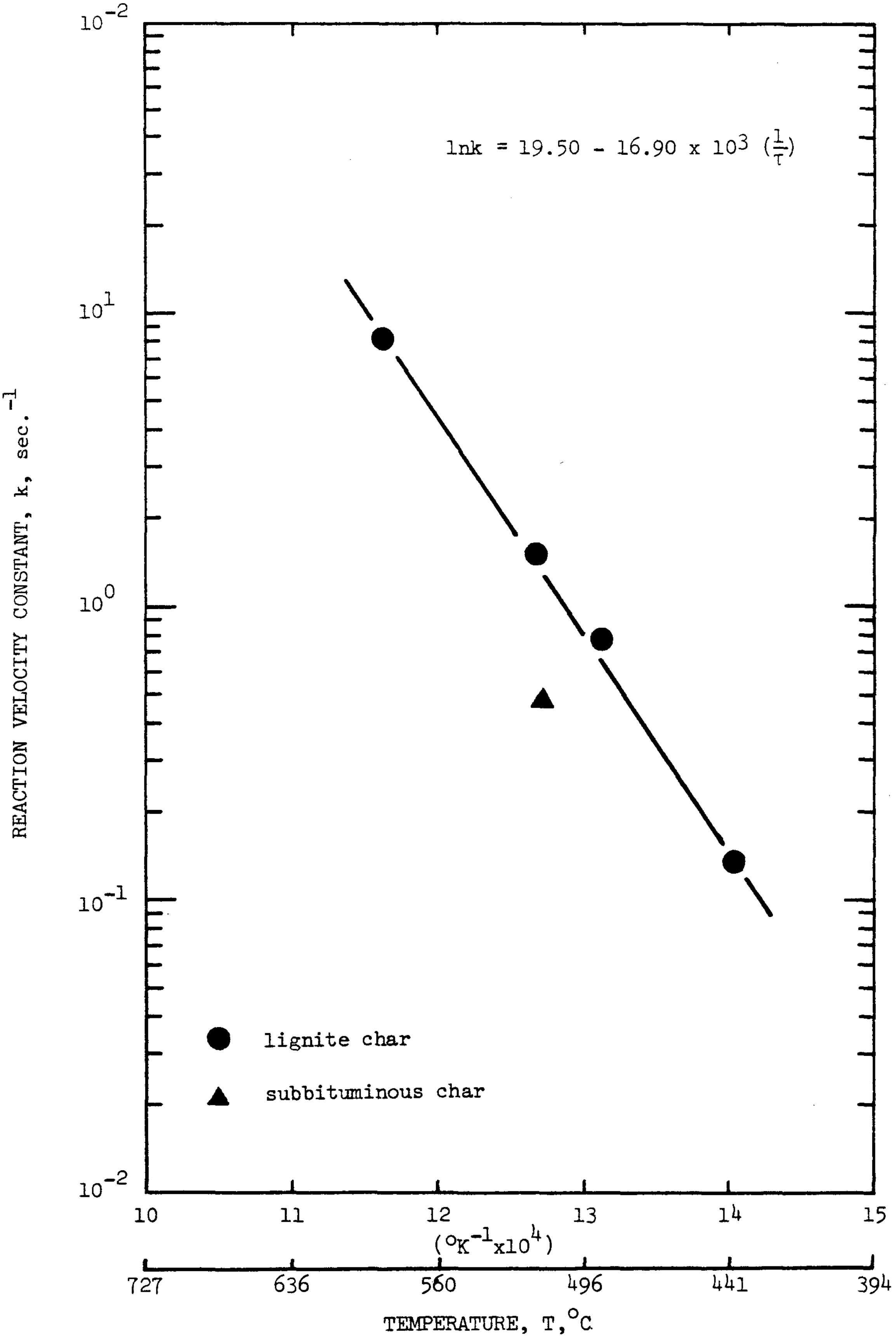

Figure 12. Arrhenius Plot for First Order Decomposition of Phenol Over Fixed Beds of Lignite and Subbituminous Char.

especially due to the difficulty inherent in performing these experiments.

Heterogeneous decomposition rate constants are compared to the homogeneous case in the same manner as done for ortho-cresol. Results of this comparison are shown in Table 7. It is evident that the presence of lignite char solids significantly increases observed rates of phenol decomposition. Assuming reliable extrapolation of the respective rate experessions into the temperature range 600-700°C, over a two order of magnitude rate enhancement is obtained in the presence of lignite char solids under these experimental conditions. These results were not surprising as approximately 300 gm. of char solids with a surface area of 360 $m.^2/gm.$ were present during experiments in which a total of 1 gm. of phenol was fed to the reactor. Thus, the potential for catalytic decomposition on the surface of the char particles was extensive. Although the mechanism for this enhanced decomposition can not be determined from these experiments, the magnitude of the catalytic effect of solids was amply demonstrated.

As was the case for lignite, subbituminous char also substantially increased phenol decomposition rates. Comparison of data from run PDR-71 and the correlated homogeneous kinetic parameters (i.e., at the run temperature of 513°C) resulted in over a 260-fold rate enhancement for phenol decomposition. This occurred in a solids environment containing approximately 300 gm. of char with a surface area of ~280 $m.^2/gm.$ Comparison of heterogeneous decomposition rates (at run PDR-71 conditions) indicated that phenol was 3 times more reactive over lignite char than subbituminous char.

Table 6. Comparative Rate Constants for Homogeneous Gas Phase Decomposition of Phenol and Ortho-Cresol

Temperature, °C	$k^{(a)}_{o\text{-cresol}}/k^{(b)}_{phenol}$
600	65
700	17
800	6
900	2

Footnotes:

(a) Data from experiments run between 475-925°C.

(b) Data from experiments run between 750-975°C (see Appendix B).

Table 7. Comparative Rate Constants for Thermal Decomposition of Phenol During Homogeneous Gas Phase and Heterogeneous Fixed Lignite Char Bed Reaction

Temperature, °C	$k^{(a)}_{hetero}/k^{(b)}_{homo}$
400	1320
500	770
600	510
700	370
800	280
900	225

Footnotes:

(a) Data from experiments run between 435-590°C.

(b) Data from experiments run between 750-975°C (see Appendix B).

It is uncertain what specific char properties were responsible for enhancing the observed decomposition of phenol. Candidate possibilities include (see Table 8):

- char surface area
- carbon and/or ash content
- specific ash constituents

It is evident that char surface area relative to that for the acceptor (i.e., 360 and 280, versus 1 $m^2/gm.$) must have played an important role. Decomposition rates are also significantly higher for lignite compared to subbituminous char, coinciding with a higher lignite surface area. This behavior corresponds with previously observed results for coal char gasification, with reactivity decreasing with coal rank (i.e., decreasing from lignite to subbituminous to bituminous chars)(30). Although carbon content is comparable on the average, ash and fixed carbon content are higher and lower, respectively, for the lignite char. Similarly, if specific ash constituents are considered (adjusted for total ash content), lignite char used in these experiments contains significantly higher fractions of Fe_2O_3, CaO, MgO, Na_2O and K_2O. Both chars contain substantial fractions of silica, Al_2O_3 and CaO. Previous studies on lignite char gasification(31) report significantly higher reactivities for unwashed chars, particularly where Na_2O is removed. While there are a variety of potential explanations for the observed enhancement of phenol acitivity by char (including that of lignite over subbituminous results), the particular explanation is not discernable from these experiments. As a preliminary estimate, coal reactivity during gasification may provide an indication of relative enhancement of phenol decomposition rates.

Table 8. Comparison of Representative Properties of Lignite and Subbituminous Chars[a]

Property	North Dakota Lignite Char	Montana Rosebud Subbituminous Char
Surface Area ($m.^2/gm.$)	357 ± 13(19)[b]	276 ± 17(4)
Composition(wt.%)		
Carbon	92.7 ± 3.0(4)	90.6
Fixed Carbon	56.4 ± 3.8(4)	65.7
Ash	32.2 ± 5.7(4)	22.6

Footnotes:

(a) Data used to make these comparisons appear in Appendix A.

(b) Average ± standard deviation for number of data points in parentheses.

Finally, results of run PDR-73 suggest both a reactivity ordering of the phenol homologues and the decreased reactivity of phenol over subbituminous char. Data from this experiment (see Table 9) show a significant shift in the distribution of phenolic compounds in the phenolic water (i.e., from CHPM-365) processed through the reactor. Total quantities of xylenols and cresols are reduced, while phenol content increased. These respective changes are more apparent when considered on a decomposition basis, as it is apparent that phenol is actually produced during this experiment. Considering decomposition results adjusted to account for sequential dehydroxylation of alkyl phenols indicates the order of reactivity as xylenols > cresols > phenol. The less predominant catalytic effect of subbituminous char in comparison to lignite char is also indicated.

Phenolic Compound Decomposition Patterns

Phenolic compounds are inherently liable to both thermal and catalytic decomposition processes, although not to the same extent. Thermal conditions typical during coal gasification are conducive to achieving significant levels of decomposition. In addition the unique gaseous atmosphere present in coal gasification (i.e., high H_2 and H_2O partial pressures), coupled with relatively small quantities of phenols, precisely determines the predominant decomposition mechanisms and pathways.

Table 9. Summary of Phenolic Compound Decomposition over Fixed Beds of Subbituminous Char During Run PDR-73.

Phenolic Compound	Condensate Composition, mg./l.		Decomposition, mol. %	
	Feed[(a)]	Product	As Received[(b)]	Adjusted[(c)]
Phenol	565	797	-41	4
Cresols	339	90	73	78
Xylenols	83	10	88	88
Total	987	897	20	-

Footnotes:

(a) Synthane PDU process condensate from Run CHPM-365.

(b) Based on measured condensate flows and reported compositions.

(c) Calculated assuming a sequential decomposition pathway from xylenols to cresols to phenol.

Relative Reactivity of Phenols

A significant base of data exists which defines the decomposition characteristics of alkyl-phenols (see decomposition mechanism discussion). In general these results indicate:

(1) as a compound class, xylenols are more reactive than cresols

(2) cresol isomer reactivity decreases in the order ortho > para > meta .

These characteristics are representative of phenolic compound decomposition studies conducted in inert (i.e., excess <20/1 on a molar basis), steam and hydrogen atmospheres, over a wide range of temperature and residence time conditions. While this behavior usually includes reactions to form both dehydroxylation and dealkylation products, it is consistent with that observed for methyl-benzene hydrodealkylation (i.e., reactivity increases with more methyl substitution).

Results of these experimental studies expands upon the state-of-the-art knowledge of phenolic compound decomposition rates. The reactivity of ortho-cresol was found to be nominally on the order of magnitude larger than that for phenol in the range 700-800°C. In light of the previous work on the isomeric cresols, the relative reactivity of ortho-cresol: meta-cresol: phenol is approximately 10:5:1. Relative to phenol, xylenol isomers are at least 15 times more reactive. In the context of thermal conditions typical in coal gasification processing, phenol is the least reactive single ring phenolic compound produced.

Phenolic Compound Decomposition Pathways

Experimental studies reported in the literature generally define the decomposition pathways for alkyl phenols. Essentially, decomposition occurs by either dealkylation or dehydroxylation for both xylenols and cresols. Obviously this implies that both toluene and cresols can be products of xylenol decomposition, with benzene and phenol as products of cresol decomposition. Production of heavy hydrocarbon tars as a secondary reaction product is minimal in atmospheres containing significant quantities of hydrogen.

Results of these experimental studies point to a more precise reaction pathway for decomposition of phenols in coal gasification. Characteristics identified from these studies include:

(1) phenol as the major product of ortho-cresol decompositon

(2) minimal production of toluene or benzene.

Apparently, this behavior is the result of excessive quantities of steam present in the reaction gas atmosphere, which act to reduce the tendency of phenols to dehydroxylate during thermal cracking. Dehydroxylation products such as toluene or benzene were rarely detected in more than trace quantities. In addition, previous phenol decomposition studies performed under conditions similar to those used here report negligible production of benzene(9).

As a result of these experimental studies, coupled with previously identified results of alkyl phenol reaction studies, the decomposition pathway for phenols (see Figure 13), consists of successive

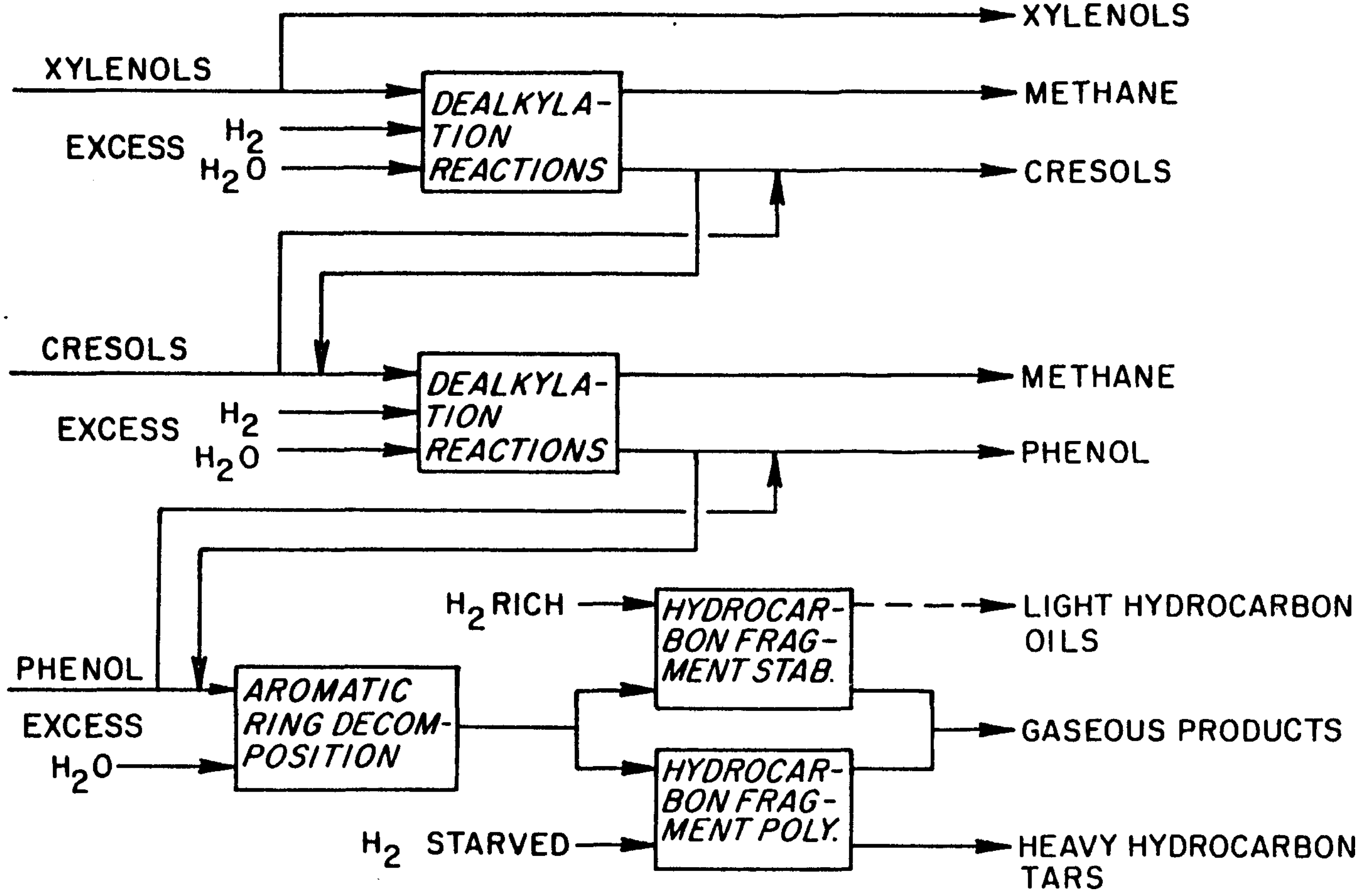

Figure 13. Pathways of Phenolic Compound Decomposition in Coal Gasification Processing.

dealkylation of methyl phenols through lower homologues to phenol. Phenol finally decomposes mainly to gaseous light hydrocarbons and carbon oxides(9), and is the rate limiting step in the decomposition sequence. Dehydroxylation of phenols to form benzene and toluene does not occur to any significant extent due to the excessive quantities of steam relative to phenols (i.e., as high as 1000/1 on a molar basis). Presence of excessive amounts of hydrogen typically present in the coal gasification environment (i.e., >100 times that of phenol on a molar basis) minimizes production of heavy hydrocarbon tars/oils as secondary decomposition products.

Application of Results to Coal Gasification Processes

The eventual usefulness of these experimental results rests in their utilization for predicting large-scale gasification process phenolic compound production patterns. Decomposition characteristics of phenols identified in this work consist of:

(1) successive dealkylation of alkyl phenols to form phenol

(2) phenol decomposition as the rate limiting step in the decomposition pathway

(3) identification of an upper bound for potential phenol decomposition over char solids.

Since formation of phenols during coal processing occurs inherently during devolatilization and is thus controlled by thermal decomposition processes(2,32-34), estimates can be made of attainable phenol decomposition during coal gasification processing. Phenol decomposition kinetics from this and previous(9) studies are applied at various coal gasification system conditions to scope predicted production patterns, and compared to trends observed from actual plant data. Processes chosen for this analysis include CO_2-Acceptor and Hygas pilot plants, and the Synthane PDU. Processing conditions important in affecting decompositiion characteristics include temperature, residence time, H_2/Phenol and H_2O/Phenol molar ratios, which are summarized in Table 10.

Data shown in Table 10 represent a number of similarities and some very drastic differences. All gasification systems have reaction atmospheres which ensure the successive phenolic compound dealkylation pathway identified in this work, and minimal production of heavy hydrocarbon condensates (i.e., excessive quantities of steam and hydrogen, respectively). However, these processes also represent distinctly different processing conditions and reaction geometries. Gas-solid contacting varies substantially, ranging from an entrained flow riser (i.e., conditions during initial coal devolatilization in the gasifier) in the Hygas reactor to two significantly different fluidized bed geometries (i.e., L/D ratios of ~7/1 and 18/1 for CO_2 Acceptor and Synthane, respectively). Temperature and residence time also varies significantly with variations seen both between and within processes for individual runs (i.e., variation with vertical position in the Synthane fluidized bed) and between runs (i.e., Hygas riser conditions). Although not noted, coals processed and pressure also vary considerably. CO_2-Acceptor and Synthane data represent processing of lignite coal, Hygas data includes processing of lignite, subbituminous and bituminous coals. Pressure levels during gasification increase from 150 psig for CO_2-Acceptor, to 600 psig for Synthane, to 1000 psig for Hygas.

Table 10. Process Conditions Which Affect Production of Phenols for the CO_2-Acceptor, Hygas, and Synthane PDU Gasifiers

Process Gasifier	Temperature, °C	Residence Time, sec (a)	H_2/Phenol, molar (b)	H_2O/Phenol, molar (b)
CO_2-Acceptor Pilot Plant (c)	815	25	500	500
Hygas Pilot Plant (d)	450-650	1	100	1000
Synthane PDU (e)	700-900	3-7	100	1000

Footnotes:

(a) Based on reactor dimensions using superficial gas velocities.

(b) Order-of-magnitude estimates based on available operating data.

(c) Representative of conditions in the fluidized bed gasifier (see reference 31), with an assumed formation of phenols of ~10 lb/ton MAF coal.

(d) Representative of conditions in the gasifier's riser tube (see reference 3).

(e) Representative of conditions in the gasifier's fluidized bed (see reference 1).

Both homogeneous and heterogeneous phenol decomposition rates were applied at temperature and vapor residence time conditions shown in Table 10 assuming plug flow of gases in each reactor. Results of this analysis are summarized in Table 11 and compared to measured phenol production for the various facilities. Results of this analysis conform with measured production patterns as follows:

(1) substantial (i.e., almost complete) decomposition of phenols released from coal occurs in the CO_2-Acceptor gasifier for both homogeneous and heterogeneous decomposition

(2) variation in heterogeneous reaction rates appears to account for measured production patterns in the Hygas gasifier

(3) phenol production in the Synthane PDU varies with homogeneous reaction rates.

The observed behavior for CO_2-Acceptor is not surprising considering the severe thermal conditions and the extensive residence time of gases in the gasifier's fluidized bed. Production of phenols predicted for Hygas is misleading, as phenol production actually increases with increasing riser temperature and decreasing vapor residence time (i.e., counter-intuitive to expected hydrocarbon decomposition characteristics)(3). However, this behavior was previously attributed to interferences caused by downstream solids removal and raw product gas quench system characteristics. Incomplete release of phenols from coal during devolatilization at lower riser temperatures might also explain this behavior. Finally, production of phenols from the Synthane PDU is significantly reduced as fresh coal is fed deeper into the gasifier's fluidized bed (i.e., effectively increasing devolatilization temperature and vapor residence time in contact with hot char solids)(1,2). The fact that production varies with

Table 11. Phenol Production Patterns for the CO_2-Acceptor, Hygas and Synthane PDU Gasifier

Process Gasifier	Phenol Production,[a] lb/ton MAF coal	Undecomposed Phenol[b], percent	
		Homogeneous	Heterogeneous
CO_2- Acceptor Pilot Plant	< 0.01	1	0
Hygas Pilot Plant	1-16	99+	19-97
Synthane PDU	1-12	1-93	0

Footnotes:

(a) See references cited in Table 1. Represents total phenols measured as phenol.

(b) Expressed as 1- fraction decomposed calculated from homogeneous and heterogeneous phenol decomposition kinetics assuming ideal plug flow.

homogeneous reaction rates may reflect differences in gas-solids contacting between those in the Synthane PDU and these experimental investigations (i.e., fluidized bed gasifier versus fixed char bed reactor).

Further Related Studies

The goals of this experimental program were to identify the reactivity of phenol relative to other phenols produced during coal gasification and to quantify the catalytic effect of gasifier solids on phenol decomposition rates. These goals were achieved by utilization of experimental data, generated in this and previous studies. However, based upon characteristics identified during generation and application of the results of this study, a few key issues require resolution:

(1) effects of variable process gas steam content on the decomposition pathway of phenols

(2) effects of type and relative quantities of solid char on phenol decomposition rates

(3) characteristics of phenolic compound formation from coal.

The effects of both steam and gasifier solids are of prime importance. Since the presence of steam appears to be necessary to maintain the successive dealkylation decomposition pathway, the precise mechanism and limits of this effect should be ascertained. This is especially critical to the proper evaluation of phenolic compound behavior in low-BTU gasification systems, which do not use reactant steam in the gasification process. In the case of a char solids, the effects of such variables as coal rank, carbon or ash content, and relative quantities of phenols and char should be determined for a more quantitative understanding of kinetics of the decomposition process. Variation of gas-solid contacting patterns during decomposition experiments might also be useful in quantifying this behavior.

Determination of patterns of phenolic compound release from coal during devolatilization is another piece of information necessary to quantitatively project production of phenols during coal gasification. Unfortunately, this is not an easy task. Results from experimental systems large enough to produce measureable quantities of phenols are inherently biased by simultaneous decomposition processes. Smaller experimental systems, while capable of decoupling formation and decomposition phenomena, typically do not produce enough material to perform accurate analytical characterizations. Such an experimental study, however, could provide insights into the range of conditions where phenols are formed from coal.

ACKNOWLEDGEMENTS

Results presented in this investigation reflect substantial cooperative efforts between Carnegie-Mellon University and a range of personnel. The authors wish to thank the Pittsburgh Energy Technology Center for their analytical support and assistance during these bench-scale studies. The authors also wish to thank the Conoco Coal Development Company for providing limestone acceptor samples and properties for this study. Finally, acknowledgment is given to various Carnegie-

Mellon University students including Marijo Andrake, Terry Hanna, Michael Pochan and Michael Rish for providing experimental, analytical and calculational support.

NOMENCLATURE

k = first order reaction velocity constant, sec.^{-1}

r_c = reaction rate, gm. mols. ortho-cresol converted/liter-sec.

r_0 = reaction rate, gm.mols. phenol converted/liter-sec.

r^2 = coefficient of determination

v_o = total volumetric feedrate, liters/sec.

A = frequency factor, sec.^{-1}

C_c = ortho-cresol concentration, gm.mols/liter

C_{co} = inlet ortho-cresol concentration, gm.mols./liter

E = activation energy, kcal./gm.mol.

F_{co} = inlet ortho-cresol molar flow, gm.mols./sec

T = temperature, ^{o}C (or ^{o}K)

V = reactor volume, liters

X_c = ortho-cresol decomposition

X_ϕ = phenol decomposition

τ = vapor residence time, sec.

(1) Nakles, D.V., M.J. Massey, A.J. Forney and W.P. Haynes, "Influence of Synthane Gasifier Conditions on Effluent and Product Gas Production", Pittsburgh Energy Research Center, U.S. Energy Research and Development Administration, Pittsburgh, PA, PERC/RI-75/6, December, 1975.

(2) Nakles, D.V., "Significance of Process Variables on Liquid Effluent Production in Coal Gasification", Ph.D. Thesis, Carnegie-Mellon University, Pittsburgh, PA (1978).

(3) Jonardi, R.J., L.J. Anastasia, M.J. Massey and R.H. Karst, "Hygas Environmental Characterization: Data Synthesis, Analysis and Interpretation - Tests 37-64", Interim Report FE-2433-25 from the Institute of Gas Technology to the U.S. Department of Energy, February, 1979.

(4) Grand Forks Energy Research Center, Quarterly Technical Progress Report, U.S. Energy Research and Development Administration, GFERC/QTR-76/5, November, 1976, pp. 16-32.

(5) Ellman, R.C., B.C. Johnson, H.H. Shobert, L.E. Paulson and M.M. Fegley, "Current Status of Studies in Slagging Fixed Bed Gasification at the Grand Forks Energy Research Center", Presented at the Ninth Biennial Lignite Symposium, Grank Fords, ND, May, 1977.

(6) Fillo, J.P. and M.J. Massey, "Analysis of RA-21 Effluent Data: GFERC Slagging Fixed Bed Gasifier", Interim Report FE-2496-24 from Carnegie-Mellon University to the U.S. Department of Energy, April, 1978.

(7) Johnson, B.D., M.M. Fegley, R.C. Ellman and L.E. Paulson, "Gasification of North Dakota Lignite in a Slagging Fixed Bed Gasifier", Grand Forks Energy Technology Center, U.S. Department of Energy (1978).

(8) Paulson, L.E., H.H. Shobert and R.C. Ellman, "Sampling, Analysis, and Characterization of Effluents from the Grand Forks Energy Research Center's Slagging Fixed-Bed Gasifier", <u>Am.Chem. Soc. Div. Fuel Preprints, 23</u>(2), 107(1978).

(9) Fillo, J.P., M.J. Massey, J.P. Strakey, D.V. Nakles and W.P. Haynes, "Decomposition Characteristics of Phenol Under Synthane Gasifier Conditions", Pittsburgh Energy Research Center, U.S. Energy Research and Development Administration, Pittsburgh, PA; PERC/RI-77/6, April, 1977.

(10) Pittsburgh Energy Research Center, Quarterly Technical Progress Report, Bureau of Mines, U.S. Department of the Interior, January-March, 1974, p.12.

(11) Finseth, D., Pittsburgh Energy Research Center, Private Communication, November, 1978.

(12) Ho, C.H., B.R. Clark and M.R. Guerin, "Direct Analysis of Organic Compounds in Aqueous By-Products from Fossil Fuel Conversion Processes: Oil Shale Retorting, Synthane Coal Gasification and COED Coal Liquefaction", J. Environ. Sci. Health, A11(7), 481(1976)

(13) White, C.M. and C.E. Schmidt, "Analysis of Volatile Polar Organics in Untreated By-Product Waters from Coal Conversion Processes", Am. Chem. Soc. Div. of Fuel Chem. Preprints, 23(2), 134(1978).

(14) Curran, G.P., Conoco Coal Development Company, Private Communication, September, 1978.

(15) Jones, B.W. and M.B. Neuworth, "Thermal Cracking of Alkyl Phenols - Mechanism of Dealkylation", Ind. Eng. Chem., 44(11), 2872(1952).

(16) Jones, B.W. and M.B. Neuworth, "Thermal Cracking of Alkyl Phenols - Conversion of High Boiling Phenols", Ind. Eng. Chem., 45(12), 2704(1953).

(17) Nakai, R., "On the Thermal Decomposition of Phenols", Bull. Chem. Soc. Japan, 5, 136(1930).

(18) Cypres, R. and C. Lejeune, "Craquage Thermique Du M-Cresol, Du Benzene, Du Toluene, Et Du Phenol Entre 650 et 850°C", Ann. Mines Begique, 7-8, 1091(1965).

(19) Cypres, R. and B. Bettens, "Mecanismes De Fragmentation Pyrolytique Du Phenol Et Des Cresols", Tetrahedron, 30, 1253(1974).

(20) Cypres, R. and B. Bettens, "La Formation De La Plupart Des Composes Aromatiques Produits Lors De La Pyrolyse Du Phenol, Ne Fait Pas Intervenir Le Carbone Porteur De La Fonction Hydroxyl", Tetrahedron, 31, 359(1975).

(21) Brackman-Danheux, C., C. Delaunois and N.C. Quyen, "A Study of the Pyrolysis of Toluene and Phenols at Low Pressure", Fuel Proc. Tech., 1, 57(1977)

(22) Wells, G.L. and R. Long, "Thermal Dealkylation-Hydrocracking of Alkyl Phenols", Ind. Eng. Chem., Process Des. Develop., 1(1), 73(1962).

(23) Davies, G.A. and R. Long, "The Kinetics of the Thermal Hydrocracking of Cresols", J. Appl. Chem., 15, 117(1965).

(24) Silsby, R.I. and E.W. Sawyer, "The Dealkylation of Alkyl Aromatic Hydrocarbons - I. The Kinetics and Mechanism of Toluene Decomposition in the Presence of Hydrogen", J. Appl. Chem., 6, 347(1956).

(25) Shull, S.E. and A.N. Hixson, "Kinetics of Thermal Hydrodealkylation of Mesitylene, m-Xylene and Toluene", Ind. Eng. Chem., Process Des. Develop., 5(2), 146(1966).

(26) Szwarc, M., "The C-H Bond Energy in Toluene and Xylenes", J. Chem. Phys., 16(2), 128(1948).

(27) Virk, P.S., L.E. Chambers and H.N. Woebke, "Thermal Hydrogasification of Aromatic Compounds", in Coal Gasification, L.G. Massey, Editor, American Chemical Society: Washington, D.C. (1974).

(28) Given, P.H., "Reactions of Alkyl Phenols Over Cracking Catalysts - I. Comparison of Catalysts and Study of Reaction Conditions", J. Appl. Chem., 7, 172(1957).

(29) Saha, N.C., N.G. Basak and A. Lahiri, "Hydrogenolysis of Higher Phenols to Lower Homologues Part I - Factors Affecting Hydrogenolysis", J. Sci. Ind. Res., 19B, 67(1960).

(30) Curran, et al., "Plant Operations Final Report - CO_2-Acceptor Process Gasification Pilot Plant, Volume 12, Book 2", Final Report FE-1734-45 to the U.S. Department of Energy from Conoco Coal Development Company, November, 1978.

(31) Curran, G.P., C.E. Fink and E. Gorin, "Kinetics of Lignite Char Gasification - Relation to CO_2-Acceptor Process", Ind. Eng. Chem. Process Des. Develop., 8(4), 559(1969).

(32) Nakles, D.V. and M.J. Massey, "Gasification Process/Environmental Characterization from Pilot Plant Data," Presented at the Environmental Fuel Conversion Technology Symposium III, Hollywood, FL, September, 1977.

(33) Fillo, J.P., "An Understanding of Phenolic Compound Production During Coal Gasification Processing", Ph.D. Thesis, Carnegie-Mellon University, Pittsburgh, PA, April, 1979.

(34) Fillo, J.P. and M.J. Massey, "Fate of Phenols During the Gasification of Coal", Proceedings of the Environmental Aspects of Fuel Conversion Technology IV, Hollywood, FL, April, 1979.

(35) Hougen, O.A., and K.M. Watson, Chemical Process Principles, J. Wiley & Sons; New York (1947), pg. 884-886.

APPENDIX A

SUMMARY OF DATA FROM BENCH-SCALE DECOMPOSITION STUDIES

Table A1. Summary of Measured Reaction Gas Compositions for Homogeneous Gas Phase and Heterogeneous Fixed Bed Phenolic Compound Decomposition Experiments

Run	Dry Gas Composition[(a)], mol%				Wet Gas Composition[(a)], mol%				
	H_2	CH_4	CO	CO_2	H_2	CH_4	CO	CO_2	H_2O
PDR-36									
Feed	44.0	9.8	9.8	36.4	20.5	4.6	4.6	17.0	53.3
Product	44.2	9.8	10.1	36.5	20.6	4.6	4.7	17.0	53.3
PDR-38									
Feed(b)	-	-	-	-	-	-	-	-	50.3
Product	44.2	9.7	9.7	36.4	22.0	4.8	4.8	18.1	50.3
PDR-39									
Feed	44.2	9.7	9.6	36.5	22.7	5.0	4.9	18.8	48.6
Product	44.0	9.8	9.8	36.3	22.6	5.0	5.0	18.7	48.6
PDR-40									
Feed	44.0	9.6	9.5	36.9	19.8	4.3	4.3	16.6	55.1
Product(c)	-	-	-	-	-	-	-	-	55.1
PDR-42									
Feed	42.3	9.7	9.6	38.4	20.1	4.6	4.6	18.2	52.5
Product(c)	-	-	-	-	-	-	-	-	52.5
PDR-43									
Feed	44.7	9.5	9.4	36.4	23.2	4.9	4.9	18.9	48.0
Product	44.5	9.5	9.4	36.4	23.1	4.9	4.9	18.9	48.0
PDR-44									
Feed	43.7	9.7	9.5	37.1	21.0	4.7	4.6	17.9	52.0
Product(c)	-	-	-	-	-	-	-	-	52.0

[illegible]

Run	Dry Gas Composition(a),mol%				Wet Gas Composition(a),mol%				
	H_2	CH_4	CO	CO_2	H_2	CH_4	CO	CO_2	H_2O
PDR-45									
Feed	45.1	9.5	9.2	36.1	22.4	4.7	4.6	17.9	50.4
Product(c)	-	-	-	-	-	-	-	-	50.4
PDR-48									
Feed(b)	-	-	-	-	-	-	-	-	51.1
Product	45.0	9.5	9.3	36.2	22.0	4.6	4.5	17.7	51.1
PDR-49									
Feed	44.6	9.7	10.0	35.7	22.3	4.8	5.0	17.8	50.0
Product	45.0	9.6	9.3	36.0	22.5	4.8	4.6	18.0	50.0
PDR-50									
Feed	44.2	9.6	9.4	36.7	22.1	4.8	4.7	18.3	50.0
Product	44.7	9.6	9.4	36.2	22.3	4.8	4.7	18.1	50.0
PDR-51									
Feed	44.5	9.4	9.1	37.0	22.5	4.8	4.6	18.7	49.4
Product	44.4	9.5	9.2	36.9	22.5	4.8	4.7	18.7	49.4
PDR-52									
Feed(b)	-	-	-	-	-	-	-	-	50.3
Product	44.8	9.5	9.0	36.7	22.3	4.7	4.5	18.2	50.3
PDR-53 (b)									
Feed	-	-	-	-	-	-	-	-	50.5
Product	44.4	9.7	9.3	36.7	22.0	4.8	4.6	18.2	50.5
PDR-55									
Feed	44.5	9.6	9.2	36.7	21.3	4.6	4.4	17.5	52.2
Product	44.2	9.6	9.6	36.6	21.1	4.6	4.6	17.5	52.2
PDR-56									
Feed	43.9	9.5	9.5	37.0	22.3	4.8	4.8	18.8	49.3
Product	44.0	9.5	9.6	36.9	22.3	4.8	4.9	18.7	49.3

Table A1. (Cont'd)

Run	Dry Gas Composition(a),mol%				Wet Gas Composition(a),mol%				
	H_2	CH_4	CO	CO_2	H_2	CH_4	CO	CO_2	H_2O
PDR-57									
Feed	44.2	9.6	9.5	36.7	23.2	5.0	5.0	19.3	47.5
Product	44.2	9.5	9.5	36.8	23.2	5.0	5.0	19.3	47.5
PDR-58									
Feed	44.0	9.5	9.5	37.0	22.1	4.8	4.8	18.6	49.8
Product	43.7	9.5	9.7	37.1	21.9	4.8	4.9	18.6	49.8
PDR-59									
Feed	44.0	9.5	9.5	37.0	22.5	4.9	4.9	18.9	48.9
Product	45.3	9.6	6.4	38.5	23.1	4.9	3.3	19.7	48.9
PDR-60									
Feed(b)	-	-	-	-	-	-	-	-	45.8
Product	44.2	9.6	8.8	37.4	24.0	5.2	4.8	20.3	45.8
PDR-61									
Feed	44.1	9.5	9.6	36.8	23.4	5.0	5.1	19.5	46.9
Product	45.5	9.3	7.3	37.8	24.2	4.9	3.9	20.1	46.9
PDR-62									
Feed	44.0	9.5	9.6	36.9	21.8	4.7	4.8	18.3	50.4
Product	46.2	10.0	10.0	33.7	22.9	5.0	5.0	16.7	50.4
PDR-63									
Feed	44.4	9.6	9.6	36.3	22.8	4.9	4.9	18.7	48.6
Product	52.8	11.4	10.9	24.7	27.1	5.9	5.6	12.7	48.6
PDR-65									
Feed	43.8	9.5	9.6	37.1	21.8	4.7	4.8	18.5	50.2
Product	43.6	9.4	7.2	39.8	21.7	4.7	3.6	19.8	50.2

Table A1. (Cont'd)

Run	Dry Gas Composition[a], mol%					Wet Gas Composition[a], mol%					
	H_2	CH_4	CO	CO_2	N_2	H_2	CH_4	CO	CO_2	H_2O	N_2
PDR-67											
Feed	44.3	9.6	9.6	36.5	-	24.6	5.3	5.3	20.3	44.4	
Product	44.0	9.6	9.4	37.0	-	24.5	5.3	5.2	20.6	44.4	
PDR-68											
Feed	37.5	8.1	8.2	32.0	14.2	26.3	5.7	5.7	22.4	29.9	10.0
Product	38.0	8.2	8.2	32.2	13.3	26.6	5.7	5.7	22.6	29.9	9.3
PDR-69											
Feed	46.4	9.0	9.1	35.5	-	23.9	4.6	4.7	18.1	48.5	
Product	47.1	8.9	8.9	35.1	-	24.3	4.6	4.6	18.1	48.5	
PDR-70											
Feed	47.2	9.0	8.9	34.8	-	23.8	4.6	4.5	17.6	49.5	
Product	47.3	9.0	8.9	34.8	-	23.9	4.6	4.5	17.6	49.5	
PDR-71											
Feed	47.2	9.0	8.9	34.9	-	25.0	4.8	4.7	18.5	47.1	
Product	47.0	9.4	8.7	34.8	-	24.9	5.0	4.6	18.4	47.1	
PDR-72											
Feed	47.1	9.0	8.9	35.0	-	23.1	4.4	4.4	17.2	51.0	
Product	47.1	9.0	8.9	34.9	-	23.1	4.4	4.4	17.1	51.0	
PDR-73											
Feed	47.5	9.0	8.9	34.5	-	25.3	4.8	4.7	18.4	46.7	
Product	47.0	9.8	8.5	34.7	-	25.0	5.2	4.5	18.5	46.7	

Footnotes:

(a) Values are normalized to eliminate air picked up during sampling (typically <1 percent).

(b) No data.

(c) Gas analyses omitted due to unrealistic values obtained, resulting from both poor sampling technique and analytical error.

Table A2. Summary of Representative Char Analyses

Synthane PDU Trial	Proximate Analysis, wt% Dry			Ultimate Analysis, wt.% MAF				
	Volatile Matter	Fixed Carbon	Ash	C	H	N	S	O[a]
CHPFL-2[b]	6.8	55.8	37.4	94.6	1.6	0.6	1.0	2.2
CHPFL-121	13.4	55.5	31.1	94.5	2.5	0.4	0.4	2.2
CHPFL-131[b]	10.9	52.9	36.2	92.9	1.9	0.9	0.7	3.6
CHPFL-147[b]	15.2	59.5	25.3	88.4	2.6	0.9	1.0	7.1
CHPFL-182[b]	12.9	57.2	29.9	95.0	1.6	0.7	2.1	0.6
CHPM-365[c]	11.7	65.7	22.6	90.6	2.3	0.8	0.6	5.7

Footnotes:

(a) Oxygen determined by difference except for CHPM-365.

(b) Composite of fraction >100 mesh used for decomposition experiments over lignite.

(c) Subbituminous char solids >100 mesh used during runs PDR-71-73.

Table A3. Representative Composition of Major Ash Constituents for Lignite and Subbituminous Chars

Ash Element	Ash Composition, wt% Ash North Dakota Lignite Char(9)	 Montana Subbituminous Char(b)
Silica	23.4	35.8
Al_2O_3	12.1	17.4
Fe_2O_3	13.4	6.0
TiO_2	0.7	1.00
CaO	23.5	26.6
MgO	9.0	4.6
Na_2O	3.7	0.3
K_2O	0.6	0.3
Sulfites	8.0	4.9

Footnotes:

(a) Solids analysis from PDR-59.

(b) Solids analysis from PDR-71.

Table A4. BET Surface Areas of Solids Used During Heterogeneous Fixed Bed Phenol Decomposition Experiments

Run	Designation(a)		Surface Area, m.^{2}/gm.
		LIGNITE CHAR	
PDR-59	I 1		346
	I 1		354
	I 2		344
	SS 1		344
	SS 1		350
	SS 2		350
	SS 2		353
PDR-60	I 1		348
	I 2		363
	SS 1		349
	SS 2		361
PDR-61	I 1		352
	I 2		353
	SS 1		362
	SS 2		374
PDR-67	SS 1		357
	SS 2		350
AVERAGES(b)	Inlet		351±6(7)
	Steady State		360±15(12)
	Total		357±13(19)
		LIMESTONE ACCEPTOR	
PDR-63	I 1		1
	SS 1		1
		SUBBITUMINOUS CHAR	
PDR-71	SS 1		146
	SS 2		287
PDR-73	I 1		266
	I 2		257
	SS 1		294
AVERAGES(b,c)	Inlet		262±6(2)
	Steady State		290±5(2)
	Total		276±17(4)

Footnotes:

(a) Designations are for solids packed into reactor before a run (I) and removed from reactor after a run (SS), with numbers used to indicate discrete samples.

(b) Statistics shown indicate averages ± one standard deviation for number of data points in parentheses.

(c) Analysis PDR-71:SS 1 not included in reported statistics.

Table A5. Summary of Rate Constants for First Order Homogeneous Gas Phase Ortho-Cresol Decomposition

Experiment	Average Temperature, °C	Residence Time, sec.[(a)]	Ortho-Cresol Decomposition, percent	Reaction Velocity Constant, sec.$^{-1}$
PDR-36	756	3.71	88.4	0.581
PDR-38	829	4.02	99.7	1.445
PDR-39	904	4.24	99.9+	1.629
PDR-40	929	4.11	99.9+	1.681
PDR-42	754	3.94	88.3	0.545
PDR-43	753	2.05	60.4	0.452
PDR-44	829	2.06	97.9	1.875
PDR-45	904	1.98	99.8	3.139
PDR-48	604	4.05	31.3	0.0927
PDR-49	528	3.97	33.3	0.102
PDR-50	478	3.81	99.3	1.302
PDR-51	429	3.93	35.8	0.113
PDR-52	680	1.97	43.9	0.293
PDR-53	604	2.02	36.9	0.228
PDR-56	701	3.98	57.3	0.214
PDR-57	482	4.11	16.4	0.0436
PDR-69	481	3.96	19.7	0.0554
PDR-70	532	4.00	18.1	0.0499

Footnote:

(a) Based on 0.897 liter reaction volume (see Figure 3).

Table A6. Summary of Rate Constants Pseudo-First Order Heterogeneous Fixed Bed Phenol Decomposition Experiments

Experiment	Average Bed Temperature, °C	Residence Time, sec.(a)	Decomposition, percent	Reaction Velocity Constant, sec.$^{-1}$
PDR-59	515	6.81	64.1	0.1504
PDR-60	439	7.47	9.5	0.01336
PDR-61	588	7.04	99.7	0.8252
PDR-62	517	7.76	13.7	0.01899
PDR-63	588	12.32	11.2	0.009642
PDR-65	490	7.88	45.5	0.07703
PDR-67	361	8.35	32.4	0.04689
PDR-71	513	7.46	30.2	0.04820
PDR-72(b)	436	6.74	-1.9	-
PDR-73	528	7.01	NA(c)	NA

Footnotes:

(a) Based on superficial gas velocity.

(b) Measured negative decomposition essentially indicates zero decomposition, implying that calculation of a corresponding rate constant is impossible.

(c) Due to presence of phenols, cresols and xylenols in feedwater, calculation of a rate constant is meaningless.

APPENDIX B

NON-ISOTHERMAL REACTION KINETICS FOR PREVIOUS PERC PHENOL DECOMPOSITION STUDIES

Phenol decomposition studies previously conducted at the Pittsburgh Energy Research Center(9) yielded kinetic results for first order homogeneous gas phase reaction. Kinetics were developed assuming an average reactor temperature within a pre-defined reaction zone. Typically, however, temperatures within the reactor deviated by as much as 15°C above the calculated average. The data were subsequently evaluated using the method of Hougen and Watson(35) for non-isothermal reactors to account for both temperature variation within the reaction zone and reaction end-effects previously assumed negligible(9). Results of this analysis are summarized in Table B1, and compared to previously calculated kinetic parameters. The essential result of this analysis (see Table B2) was to significantly raise the equivalent reactor volumes at the assumed base temperatures.

Results of homogeneous gas phase phenol decomposition experiments conducted during the present study (i.e., PDR-55,58 and 68) were compared with projections of kinetic constants and phenol decomposition calculated using the re-worked kinetic parameters. This comparison, shown in Table B3, indicates good correspondence with results from the previous experimental program.

Table B1. Comparison of Homogeneous Gas Phase Phenol Decomposition Kinetic Parameters for Isothermal and Non-Isothermal Reaction

Temperature Assumption	Kinetic Parameters[(a)]	
	ln A	E,kcal./gmol.
Isothermal[(b)]	20.5	38.8
Non-Isothermal	16.5	39.1

Footnotes:

(a) Calculated for runs from 750 to 950°C, excluding run PDR-21 due to analytical difficulties.

(b) Source of data is reference 9.

Table B2. Summary of Kinetic Data For First Order Homogeneous Gas Phase Decomposition of Phenol

Experiment	Base Temperature[(a)], °C	Reactor Volume[(b)], cm^3	Residence Time[(c)], sec	k, sec^{-1}
PDR-3[(d)]	600	1026	4.73	0.00931
PDR-4[(d)]	825	1026	4.60	0.243
PDR-5[(d)]	900	1026	4.77	0.728
PDR-6	900	1123	5.27	0.647
PDR-7	750	1017	4.80	0.0416
PDR-10	900	1011	4.81	0.859
PDR-11	900	1016	5.21	0.686
PDR-12	900	1027	4.63	0.680
PDR-13	900	1012	5.85	0.573
PDR-14	900	1005	4.63	0.724
PDR-15	975	977	4.44	1.193
PDR-16	825	1019	4.61	0.183
PDR-17[(d)]	750	1026	4.60	0.0652
PDR-18	825	927	2.91	0.233
PDR-19	825	1069	3.55	0.208
PDR-20	825	1018	5.28	0.175
PDR-21	825	1029	4.68	0.134
PDR-22	825	1027	4.56	0.223
PDR-23	825	1028	2.45	0.225
PDR-24	900	[illegible]	2.30	1.048
PDR-25	750	1050	4.75	0.0608
PDR-26	750	1076	2.39	0.0771
PDR-27	825	1048	2.33	0.258
PDR-28	975	968	2.18	2.671
PDR-30	825	1023	4.59	0.209
PDR-31	900	1005	2.29	1.136
PDR-32	750	1149	2.58	0.0811

Footnotes:

(a) Base temperature chosen below observed maximum temperature in temperature profile.

(b) Equivalent reactor volume determined via method of Hougen and Watson(35).

(c) Time reaction gases in equivalent reactor volume at base temperature.

(d) Lack of accurate temperature profile required using average of 1126±32 cm^3, from remaining 23 experiments.

Table B3. Comparison of Current Homogeneous Gas Phase Decomposition Results With Previously Identified Reaction Behavior

		Reaction Velocity Constant, sec.$^{-1}$		Decomposition,%	
Experiment	Base Temperature, °C	Experimental[(a)]	Predicted[(b)]	Experimental[(a)]	Predicted[(b)]
PDR-55	825	0.256	0.229	74.7	70.7
PDR-58	750	0.0684	0.0615	30.2	27.6
PDR-68	825	0.263	0.229	52.1	47.3

Footnotes:

(a) Results of the current experimental program.

(b) Based on experimental results in reference 9, using kinetic parameters developed in this appendix.

S GOVERNMENT PRINTING OFFICE: 1980-640-258 2230